



Effect of a Squeezed Vacuum on Coherent Population Trapping in a Three-level Lambda System

M.R. Ferguson , Z. Ficek & B.J. Dalton

To cite this article: M.R. Ferguson , Z. Ficek & B.J. Dalton (1995) Effect of a Squeezed Vacuum on Coherent Population Trapping in a Three-level Lambda System, Journal of Modern Optics, 42:3, 679-706, DOI: [10.1080/09500349514550621](https://doi.org/10.1080/09500349514550621)

To link to this article: <https://doi.org/10.1080/09500349514550621>



Published online: 01 Mar 2007.



Submit your article to this journal [↗](#)



Article views: 52



Citing articles: 13 View citing articles [↗](#)

Effect of a squeezed vacuum on coherent population trapping in a three-level lambda system

M. R. FERGUSON†, Z. FICEK† and B. J. DALTON†‡

†Department of Physics, The University of Queensland, Brisbane, Queensland 4072, Australia

‡Blackett Laboratory, Imperial College of Science, Technology and Medicine, London SW7 2BZ, England

(Received 23 June 1994; revision received 24 August 1994)

Abstract. Master equation methods are used to investigate the effects of a broad-band squeezed vacuum on a three-level atom of the lambda configuration. The two-mode squeezed vacuum is treated as a Markovian reservoir in a non-stationary phase-dependent state. In addition to the squeezed vacuum the atom is driven by two coherent laser fields each of which, depending on the polarization, can couple to one or both of the atomic transitions. We show that in general the optical Bloch equations for the atomic density matrix elements have oscillatory coefficients, thereby necessitating the use of Floquet methods. For the case of equal laser frequencies, which are also equal to the carrier frequency of the squeezed vacuum, the coefficients of the Bloch equations become time independent and stationary solutions for the populations and coherences are obtained by standard matrix methods. For the ordinary vacuum the usual coherent population trapping effect at two-photon resonance is obtained, with the upper state population being zero. An unsqueezed thermal field partially destroys the trapping effect as the upper state population is no longer zero at two-photon resonance. The squeezed vacuum has the effect of improving the trapping in that the coherence hole becomes more pronounced for some values of the relative phase between the squeezed vacuum and the driving fields. The additional effects of a coherence transfer rate between the two optical coherences, which occurs for special choices of angular momentum quantum numbers are also studied. For the case of equal laser frequencies, the inclusion of this coherence transfer process destroys population trapping and reduces the lambda system to a two-level system. However, for the case of unequal laser frequencies, the coherence transfer process in combination with the squeezed vacuum can restore to some extent the population trapping. We show that other features that do not occur for two-level atoms, such as stationary population inversions between pairs of the atomic levels, also depend on the relative phase and can be enhanced in the squeezed vacuum. In the case of unequal frequencies of the driving fields the population in the upper state depends on the relative phase only when the carrier frequency of the squeezed vacuum is equal to one of the two frequencies of the driving fields. When the carrier frequency of the squeezed vacuum is slightly detuned from both frequencies of the driving fields, the population in the upper state is insensitive to the relative phase but is dependent on the degree of squeezing. For large detunings, the population does not show any dependence on the degree of squeezing and its distribution in function of the two-photon detuning is similar to that in the thermal vacuum field.

1. Introduction

With the recent successful generation of squeezed light (for recent reviews, see for example [1]), a great deal of attention has been given to possible applications to

atomic spectroscopy. The reason for this is that squeezed light is an example of a non-classical state of the electromagnetic field. For the ordinary vacuum, the fluctuations (noise) in the two non-commuting field quadratures are distributed symmetrically between the two quadratures and the variance of the field quadratures is equal to their commutator establishing the level of quantum noise (vacuum fluctuations). In a squeezed vacuum the quantum fluctuations in one quadrature component are reduced below their vacuum level at the expense of increased fluctuations in the other component, such that the uncertainty relation is not violated. This modification of the quantum fluctuations has opened up many new possibilities in quantum physics and has led to predictions of novel and unusual effects. Of particular interest are those situations in which the introduction of a squeezed light source produces qualitatively different spectroscopic features to those which occur in its absence. The interaction of squeezed light with atomic systems has been recently reviewed [2]. As yet, few experiments have been performed [3] and other possible experimental situations have also been discussed in [2].

The first investigations related to two-level atoms and dealt with broad-band squeezed light. Gardiner [4] has shown that a strongly squeezed vacuum field can inhibit decay of one of the atomic polarization quadratures of a two-level atom. This modification opens the possibility of obtaining subnatural linewidths in resonance fluorescence [5] and in the weak-field atomic absorption spectrum [6]. A variety of other effects emphasizing the novel features of the interaction between two-level atoms and squeezed vacuum field have also been predicted. Examples include squeezing-induced transparency [7], level shifts [8–11], asymmetric fluorescence spectra [12] and amplification without population inversion [13].

The effects of a broad-band squeezed vacuum on three-level atoms have also been examined [14–16]. These show some very interesting deviations from the ordinary decay and ordinary fluorescence spectra. In particular, in a three-level atom in the cascade configuration interacting with a squeezed vacuum field, there are spectacular qualitative changes in the steady-state level populations relative to the ordinary vacuum, including two-photon population inversions [14–16]. Moreover, the equally spaced cascade system may generate pairwise atomic squeezed states, and a new class of states, which satisfy the equality sign in the Heisenberg uncertainty relation for angular momentum operators, called intelligent spin coherence states [15].

Further work has also been done to incorporate the effect of the broad-band squeezed vacuum on the resonance fluorescence from three-level atoms driven by two independent laser beams [17–19]. The results show that the relative heights and widths of the peaks in the fluorescence spectra can be subnatural or supernatural depending on the relative phase between the driving fields and squeezed vacuum, in a similar way as in two-level atoms. They have also examined the effect of squeezed vacua on the coherent population trapping. It is well known that, in the ordinary vacuum, population trapping is possible in a three-level atom in the lambda configuration when the lasers are exactly on the two-photon resonance with the initial and final states of the system [20–22]. When this occurs, the population is trapped in a coherent superposition of the lower states with the upper state population being zero. In the squeezed vacuum, however, the coherent population-trapping effect is reduced [18, 19].

In previous studies of the effects of the squeezed vacuum on the spectral and dynamical processes in three-level atoms it has been assumed that the atoms are

interacting with two independent broad-band squeezed vacua each of which is coupled only to one of the two possible one-photon transitions. This is equivalent to assuming that the bandwidth Γ_{sv} of the squeezed vacuum is much smaller than the difference Δ between the frequencies of the atomic transitions. In practice this condition may not always be satisfied. Finite bandwidth effects have been studied for two-level atom spontaneous emission [23], probe absorption [24] and fluorescence spectra [25].

In this paper we examine the effect of a *single* broad-band squeezed vacuum on the stationary populations and coherences in a three-level atom of the lambda configuration. We assume that Γ_{sv} is much larger than Δ . In this case the squeezed vacuum couples to both atomic transitions. In addition to the squeezed vacuum the atom is driven by two coherent laser fields, each of which is coupled to one of the two possible transitions. This could be achieved by a suitable choice of laser field polarization. We show that in general the optical Bloch equations (Floquet-type equations) for the density matrix elements have oscillating coefficients, thereby necessitating the use of continued-fraction methods. For the case of two equal laser frequencies, which are also equal to the carrier frequency of the squeezed vacuum, the Bloch equations become time independent, and steady-state solutions for the populations and coherences are obtained by standard matrix methods. The coefficients of the Bloch equations also become effectively independent of time when the carrier frequency of the squeezed vacuum is equal to the frequency of one of the two driving laser fields which significantly differs from the other frequency. In this case the Bloch equations contain time-dependent terms oscillating with frequency difference between the two laser frequencies. When the frequency difference is large, these rapidly oscillating terms can be neglected. A similar situation arises when the carrier frequency equals the average of the two laser frequencies, assuming that these are rather different. We show that in general the coherent population-trapping effect, reduced by thermal fluctuations, can be improved when the atom is in the squeezed vacuum, and the population in the upper state can exhibit a strong dependence on the phase when the laser fields are not in the two-photon resonance with the atomic transitions. The additional effects of a coherence transfer rate between the two optical coherences, which occurs for special choices of angular momentum quantum numbers are also studied. For the case of equal laser frequencies, the inclusion of this coherence transfer process destroys population trapping and can reduce the three-level atom dynamics to those characteristic of a two-level system. However, for the case of unequal laser frequencies, the coherence transfer process in combination with the squeezed vacuum can restore population trapping in part.

The plan of this paper is as follows. In section 2 the system model is described and the master equation obtained. Details of the derivation are given in appendix B, based on the general derivation for the master equation with a non stationary reservoir set out in appendix A. The Bloch equations for the atomic density matrix elements are presented in section 3. The long-time steady-state behaviour of the atomic populations and coherences is examined in section 4 for the various cases described above and conclusions drawn in section 5.

2. Master equation for three-level system in squeezed vacuum

Consider a three-level atom in the lambda (Λ) configuration with states $|1\rangle$, $|2\rangle$ and $|3\rangle$ having energies E_1 , E_2 and E_3 respectively ($E_2 > E_1$, E_3). The atom is driven classically by two coherent laser fields of frequencies ω_a and ω_b coupled to

the 1-2 and 3-2 transitions (figure 1). The transition frequencies between the ground state $|1\rangle$ and the upper state $|2\rangle$, and between the ground state $|3\rangle$ and the state $|2\rangle$ are ω_{21} and ω_{23} respectively. These transitions are associated with electric dipole matrix elements μ_{12} and μ_{32} respectively, whereas the 1-3 transition is forbidden in the electric dipole approximation ($\mu_{13} = 0$). Simultaneously, the atom is coupled to all other modes of the electromagnetic field, which are assumed to be in a broad-band squeezed vacuum state. In the electric dipole approximation the Hamiltonian of the system has the following form:

$$H = H_S + H_R + H_{RS}, \quad (1)$$

where

$$H_S = H_{SO} + H_{SL} \quad (2)$$

is the system (atom + driving fields) Hamiltonian, with

$$H_{SO}|i\rangle = E_i|i\rangle, \quad i = 1, 2, 3, \quad (3)$$

and $E_i - E_j = \hbar\omega_{ij}$,

$$H_{SL} = -\frac{1}{2}\hbar[|\Omega_a\rangle\langle 2| \exp[-i(\omega_a t + \varphi_a)] + |\Omega_b\rangle\langle 2| \exp[-i(\omega_b t + \varphi_b)]] + \text{H.c.} \quad (4)$$

is the atom-laser fields interaction Hamiltonian, where $\Omega_a = (\mu_{21} \cdot \mathbf{E}_a)/\hbar$ and $\Omega_b = (\mu_{32} \cdot \mathbf{E}_b)/\hbar$ are the Rabi frequencies of the driving laser fields of amplitudes \mathbf{E}_a and \mathbf{E}_b respectively, φ_a and φ_b are the phases associated with the corresponding Rabi frequencies. Thus $\Omega_c = |\Omega_c| \exp(-i\varphi_c)$ ($c = a, b$).

In equation (1), H_R is the Hamiltonian of the quantized electromagnetic field:

$$H_R = \hbar \sum_{\lambda} \omega_{\lambda} (a_{\lambda}^{\dagger} a_{\lambda} + \frac{1}{2}), \quad (5)$$

where a_{λ} and a_{λ}^{\dagger} are the bosonic operators for the field, and H_{RS} is the system-reservoir coupling Hamiltonian:

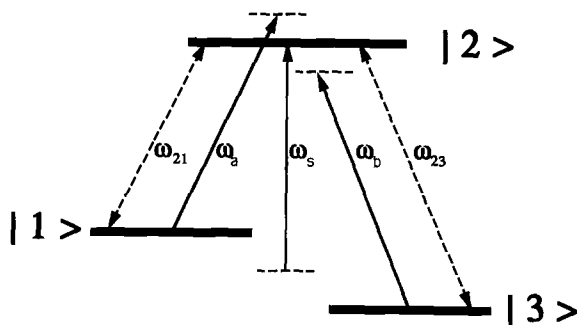


Figure 1. Schematic diagram of a three-level lambda system driven by two coherent laser fields of frequencies ω_a and ω_b , and coupled to a squeezed vacuum of the carrier frequency ω_s .

$$H_{\text{RS}} = -\frac{1}{2}i\hbar \left(\sum_{\lambda} (|2\rangle\langle 1| + |1\rangle\langle 2|) [\Omega_{\lambda}^{(1)} a_{\lambda} - (\Omega_{\lambda}^{(1)})^* a_{\lambda}^{\dagger}] \right. \\ \left. + \sum_{\lambda} (|2\rangle\langle 3| + |3\rangle\langle 2|) [\Omega_{\lambda}^{(3)} a_{\lambda} - (\Omega_{\lambda}^{(3)})^* a_{\lambda}^{\dagger}] \right), \quad (6)$$

where

$$\Omega_{\lambda}^{(1)} = (\mu_{21} \cdot \hat{\mathbf{e}}_{\lambda}) \left(\frac{2\omega_{\lambda}}{\hbar\epsilon_0 V} \right)^{1/2} \quad (7)$$

and

$$\Omega_{\lambda}^{(3)} = (\mu_{23} \cdot \hat{\mathbf{e}}_{\lambda}) \left(\frac{2\omega_{\lambda}}{\hbar\epsilon_0 V} \right)^{1/2} \quad (8)$$

are the usual one-photon Rabi frequencies of the vacuum field, $\hat{\mathbf{e}}_{\lambda}$ is the unit polarization vector, and $\lambda \equiv \mathbf{k}s$ contains the propagation vector \mathbf{k} and the polarization s .

The time evolution of the atomic system driven by coherent laser fields and simultaneously coupled to a squeezed reservoir is given as usual by the master equation of the reduced density operator of the three-level system. The details of the derivation of this master equation are given in appendix B. The master equation is based on the Born-Markoff approximations together with the secular approximation [26] (rotating-wave approximation of the second kind). In the Schrödinger picture the master equation is given by

$$\frac{\partial}{\partial t} \rho = -\frac{i}{\hbar} [H_0, \rho] + (N+1) \sum_{i,j} \Gamma_{ij} ([S_i^-, \rho S_j^+] + [S_i^- \rho, S_j^+]) + N \sum_{i,j} \Gamma_{ij} ([S_i^+, \rho S_j^-] \\ + [S_i^+ \rho, S_j^-]) + M \sum_{i,j} \Gamma_{ij} ([S_i^+, \rho S_j^+] + [S_i^+ \rho, S_j^+]) \exp(-2i\omega_s t) \\ + M^* \sum_{i,j} \Gamma_{ij} ([S_i^-, \rho S_j^-] + [S_i^- \rho, S_j^-]) \exp(2i\omega_s t), \quad (9)$$

where

$$H_0 = \hbar\omega_{23}|2\rangle\langle 2| + \hbar(\omega_{23} - \omega_{21})|1\rangle\langle 1| - \frac{1}{2}\hbar[\Omega_a S_1^+ \exp(-i\omega_a t) + \Omega_a^* S_1^- \exp(+i\omega_a t)] \\ - \frac{1}{2}\hbar[\Omega_b S_3^+ \exp(-i\omega_b t) + \Omega_b^* S_3^- \exp(+i\omega_b t)], \quad (10)$$

with $S_1^+ = |2\rangle\langle 1|$, $S_1^- = |1\rangle\langle 2|$, $S_3^+ = |2\rangle\langle 3|$ and $S_3^- = |3\rangle\langle 2|$. The sum over i, j is with $i, j = 1, 3$ only. The parameters $N = N(\omega_s)$ and $M = |M(\omega_s)| \exp(i\varphi_s)$ characterize squeezing such that $|M|^2 \leq N(N+1)$, where the equality holds for the minimum-uncertainty squeezed states, ω_s is the carrier frequency of the squeezed vacuum and φ_s is its phase. In equation (9) we have assumed that $N(\omega_{21}) = N(\omega_{23}) = N(\omega_s)$ and $M(\omega_{21}) = M(\omega_{23}) = M(\omega_s)$. Also we have assumed that (i) the dipole matrix elements are real, (ii) the intensity dependent Lamb shifts A_{ij}^+ and A_{ij}^- can be ignored and (iii) the other squeezing parameter ΔM_{ij} can be neglected (see [14]).

The parameters Γ_{11} and Γ_{33} which appear in equation (9) are the rates for spontaneous emission from the state $|2\rangle$ to the states $|1\rangle$ and $|3\rangle$ (see equations

(B 21) and (B 22)), respectively. $\Gamma_{ij}(i \neq j)$ are the coherence transfer rates which couple the 1-2 and 3-2 atomic coherences (see equation (B23)):

$$\Gamma_{13} = \Gamma_{31} = \frac{\mu_{12} \mu_{32}}{6\pi\epsilon_0 \hbar c^3} (\omega_{21}^3 + \omega_{23}^3). \quad (11)$$

Evaluation of Γ_{13} produces the following selection rules in terms of angular momentum quantum numbers: $J_2 - J_1 = \pm 1, 0$, $J_2 - J_3 = \pm 1, 0$, and $M_2 - M_1 = M_2 - M_3 = \pm 1, 0$. Since in many atomic systems $M_1 \neq M_3$, then $\Gamma_{13} = 0$ and the atomic coherences 1-2 and 3-2 are independent. In spite of this, the effect of Γ_{13} on the radiative processes in the lambda system has been recently discussed [15, 26, 27] with overall conclusion that, even with incoherent pumping, novel effects such as quantum beats may occur in the system when $\Gamma_{13} \neq 0$. In this paper we discuss the effect of Γ_{13} on the coherent population trapping and show that, in the squeezed vacuum, $\Gamma_{13} \neq 0$ can lead to a transfer of correlations from the squeezed vacuum to the atomic system.

3. Atomic Bloch equations

Having established the atomic master equation in operator form, we can obtain Bloch equations for the atomic density matrix elements. The Hamiltonian H_0 , appearing in the master equation (9), contains explicit time-dependent factors of the complex exponential type. These can be removed by translating the density matrix elements to a frame rotating with the laser frequencies

$$\begin{aligned} \tilde{\rho}_{12} &= i\rho_{12} \exp[-i\omega_a t] = \tilde{\rho}_{21}^*, \\ \tilde{\rho}_{32} &= i\rho_{32} \exp[-i\omega_b t] = \tilde{\rho}_{23}^*, \\ \tilde{\rho}_{13} &= \rho_{13} \exp[-i(\omega_a - \omega_b)t] = \tilde{\rho}_{31}^*. \end{aligned} \quad (12)$$

For simplicity we have set the laser phases φ_a, φ_b to zero. Noting that $\tilde{\rho}_{11} + \tilde{\rho}_{22} + \tilde{\rho}_{33}$ is independent of time and equal to unity, the equations of motion for the density matrix elements $\tilde{\rho}_{ij}$ are

$$\begin{aligned} \dot{\tilde{\rho}}_{11} &= -N\gamma_1 \tilde{\rho}_{11} + (N+1)\gamma_1 \tilde{\rho}_{22} + \frac{1}{2}\xi_a(\tilde{\rho}_{12} + \tilde{\rho}_{21}) - \frac{1}{2}N\gamma_{13}[\tilde{\rho}_{13} \exp(i\Delta_0 t) \\ &\quad + \tilde{\rho}_{31} \exp(-i\Delta_0 t)], \\ \dot{\tilde{\rho}}_{22} &= N\gamma_3 + N(\gamma_1 - \gamma_3)\tilde{\rho}_{11} - [(N+1) + N\gamma_3]\tilde{\rho}_{22} - \frac{1}{2}\xi_a(\tilde{\rho}_{12} + \tilde{\rho}_{21}) - \frac{1}{2}\xi_b(\tilde{\rho}_{32} + \tilde{\rho}_{23}) \\ &\quad + N\gamma_{13}[\tilde{\rho}_{13} \exp(i\Delta_0 t) + \tilde{\rho}_{31} \exp(-i\Delta_0 t)], \\ \dot{\tilde{\rho}}_{12} &= -\{i(\Delta_T + \delta) + \frac{1}{2}[N\gamma_1 + (N+1)]\}\tilde{\rho}_{12} - \frac{1}{2}\xi_b \tilde{\rho}_{13} - \frac{1}{2}\xi_a(\tilde{\rho}_{11} - \tilde{\rho}_{22}) - M^* \gamma_1 \tilde{\rho}_{21} \\ &\quad \times \exp[-i(\Delta_0 - \Delta)t] - \gamma_{13}[\frac{1}{2}N\tilde{\rho}_{32} \exp(-i\Delta_0 t) + M^* \tilde{\rho}_{23} \exp(i\Delta t)], \\ \dot{\tilde{\rho}}_{32} &= -\frac{1}{2}\xi_b + \{i(\Delta_T - \delta) - \frac{1}{2}[(N+1) + N\gamma_3]\}\tilde{\rho}_{32} - \frac{1}{2}\xi_a \tilde{\rho}_{31} + \frac{1}{2}\xi_b(2\tilde{\rho}_{22} + \tilde{\rho}_{11}) \\ &\quad - M^* \gamma_3 \tilde{\rho}_{23} \exp[i(\Delta_0 + \Delta)t] - \gamma_{13}[\frac{1}{2}N\tilde{\rho}_{12} \exp(i\Delta_0 t) + M^* \tilde{\rho}_{21} \exp(i\Delta t)], \\ \dot{\tilde{\rho}}_{13} &= -(2i\Delta_T + \frac{1}{2}N)\tilde{\rho}_{13} + \frac{1}{2}\xi_b \tilde{\rho}_{12} + \frac{1}{2}\xi_a \tilde{\rho}_{23} + \frac{1}{2}\gamma_{13}[(3N+2)\tilde{\rho}_{22} - N] \exp(-i\Delta_0 t), \end{aligned} \quad (13)$$

where the dot refers to differentiation with respect to $(\Gamma_{11} + \Gamma_{33})t$, and

$$\gamma_1 = \frac{\Gamma_{11}}{\Gamma_{11} + \Gamma_{33}}, \quad \gamma_3 = \frac{\Gamma_{33}}{\Gamma_{11} + \Gamma_{33}}, \quad \gamma_{13} = \frac{\Gamma_{13}}{\Gamma_{11} + \Gamma_{33}},$$

$$\begin{aligned}
 \xi_a &= \frac{|\Omega_a|}{\Gamma_{11} + \Gamma_{33}}, \quad \xi_b = \frac{|\Omega_b|}{\Gamma_{11} + \Gamma_{33}}, \\
 \Delta_0 &= \frac{\omega_a - \omega_b}{\Gamma_{11} + \Gamma_{33}}, \quad \Delta = \frac{2\omega_s - \omega_a - \omega_b}{\Gamma_{11} + \Gamma_{33}}, \\
 \Delta_T &= \frac{\frac{1}{2}(\omega_a - \omega_b + \omega_{23} - \omega_{21})}{\Gamma_{11} + \Gamma_{33}}, \quad \delta = \frac{\frac{1}{2}(\omega_a + \omega_b - \omega_{21} - \omega_{23})}{\Gamma_{11} + \Gamma_{33}},
 \end{aligned}
 \tag{14}$$

are dimensionless parameters for the atomic decay rates γ_1 and γ_3 , the coherence transfer rate γ_{13} , the Rabi frequencies ξ_a and ξ_b of the laser field having a difference frequency Δ_0 and two-photon detuning Δ_T . The parameter Δ describes the relation between the centre frequency of the squeezed vacuum and the average of the driving frequencies and δ determines the average one-photon detuning.

The equations of motion for the remaining off-diagonal density matrix elements $\tilde{\rho}_{21}$, $\tilde{\rho}_{23}$ and $\tilde{\rho}_{31}$ can be obtained from equation (13) by complex conjugation.

It is seen from equation (13) that for $\omega_a \neq \omega_b$ the coefficients of the equations of motion for the density matrix elements depend on time. It is not difficult to show that for both $\omega_a \neq \omega_s$, $\omega_b \neq \omega_s$ and $\Omega_a, \Omega_b \neq 0$ a rotating frames *does not* exist for which the coefficients would be time independent. Only for $\Omega_a, \Omega_b = 0$ or for both $\Omega_a, \Omega_b \neq 0$ and $\omega_a = \omega_b = \omega_s$ is it possible to find a rotating frame in which the coefficients are independent of time. The situation of the equations of motion with time-independent coefficients is also obtainable when, instead of one squeezed vacuum coupled to both transitions, one uses two squeezed vacua each of which is coupled to only one of the two possible transitions and centred around the laser frequencies [17–19]. In this case the equations of motion for the density matrix elements can be solved analytically. When one squeezed vacuum coupled to both transitions is used and $\omega_s \neq \omega_a, \omega_b$, the equations of motion have no general analytical solution and some approximations need to be used.

4. Long-time steady-state behaviour of atomic populations and coherences

4.1. Case when $\omega_a = \omega_b = \omega_s$: Steady-state solutions

We first look at the case of the steady-state solutions of the equations of motion (13) when $\omega_a = \omega_b = \omega_s$, that is both driving laser fields have the same frequency equal to the carrier frequency of the squeezed vacuum. In this limit $\Delta_0 = \Delta = 0$, and the coefficients of the equations (13) become time independent and steady (constant) long-time solutions can be obtained.

By setting the left-hand side of equations (13) equal to zero we obtain the steady-state solutions for the density matrix elements. We now focus on the steady-state population in the upper state $|2\rangle$ for different types of reservoir to which the three-level system can be coupled.

4.1.1. Reservoir at zero temperature (ordinary vacuum)

For a zero-temperature reservoir, $N = |M| = 0$, and equation (13) reduces to the well known optical Bloch equations of a three-level system driven by two laser fields and damped by the ordinary vacuum [20, 21]. Figure 2 shows the stationary population of the upper state $|2\rangle$ as a function of the two-photon detuning Δ_T for

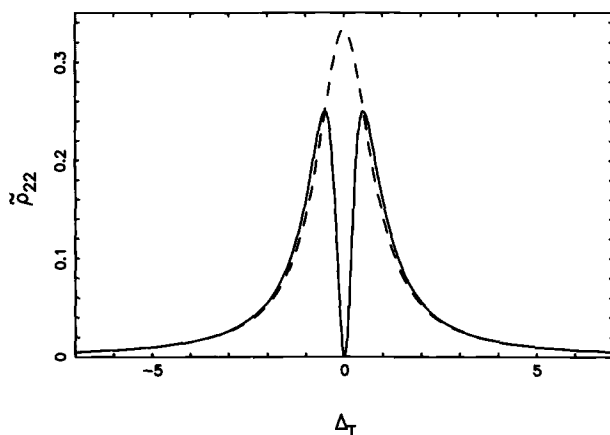


Figure 2. Stationary population of the upper state $|2\rangle$ in the ordinary vacuum as a function of the two-photon detuning Δ_T for $N=|M|=0$, $\delta=0$, $\Delta_0=\Delta=0$, $\xi_a=\xi_b=1$, $\gamma_1=\gamma_3=0.5$ and different γ_{13} : (—), $\gamma_{13}=0$; (---), $\gamma_{13}=0.5$.

$N=|M|=0$, $\delta=0$, equal normalized Rabi frequencies $\xi_a=\xi_b=1$, equal decay rates $\gamma_1=\gamma_3=0.5$, and different values of the coherent transfer rate γ_{13} . It is seen that for $\gamma_{13}=0$ the state $|2\rangle$ is not populated when the driving laser fields are exactly in two-photon resonance with the atomic transitions. This phenomenon, known as coherent population trapping (CPT), has been extensively discussed in the literature [20–22] and shows that in the lambda system the population can be trapped in the ground states $|1\rangle$ and $|3\rangle$. As it is seen from figure 2 the CPT effect strongly depends on the coherence transfer rate and disappears when $\gamma_{13}\neq 0$. The CPT effect and its dependence on γ_{13} can be explained by examining the population dynamics in new states $|S\rangle$ and $|A\rangle$, which are linear superpositions of the ground states $|1\rangle$ and $|3\rangle$:

$$\begin{aligned}
 |S\rangle &= \frac{1}{2^{1/2}}(|1\rangle + |3\rangle), \\
 |A\rangle &= \frac{1}{2^{1/2}}(|1\rangle - |3\rangle).
 \end{aligned}
 \tag{15}$$

From equations (13) and (15), we find that

$$\begin{aligned}
 \dot{\rho}_{AA} &= \langle A|\dot{\rho}|A\rangle \\
 &= \frac{1}{2}\{N(\gamma_{13}-\gamma_3)(1-\tilde{\rho}_{22}) + N(\gamma_3-\gamma_1)\tilde{\rho}_{11} + 2i\Delta_T(\tilde{\rho}_{13}-\tilde{\rho}_{31}) + (\gamma_1+\gamma_3-2\gamma_{13}) \\
 &\quad \times [(N+1)\tilde{\rho}_{22} + \frac{1}{2}N(\tilde{\rho}_{13}+\tilde{\rho}_{31})]\} - \frac{1}{2}(\xi_a-\xi_b)(\tilde{\rho}_{12}+\tilde{\rho}_{21}-\tilde{\rho}_{32}-\tilde{\rho}_{23})\}.
 \end{aligned}
 \tag{16}$$

In the case of a zero-temperature reservoir, $N=|M|=0$, and for $\xi_a=\xi_b$ at $\Delta_T=0$, we obtain

$$\dot{\rho}_{AA} = \frac{1}{2}(\gamma_1+\gamma_3-2\gamma_{13})\tilde{\rho}_{22},
 \tag{17}$$

which indicates that in the steady state ($\dot{\rho}_{AA}=0$) the population $\tilde{\rho}_{22}=0$ unless $\gamma_1+\gamma_3-2\gamma_{13}=0$ and the $\tilde{\rho}_{22}\neq 0$. The latter happens when $\gamma_1=\gamma_3=2\gamma_{13}$ and shows

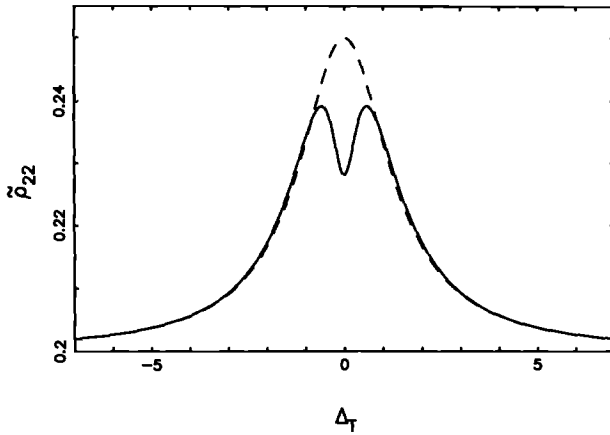


Figure 3. Stationary population of the upper state $|2\rangle$ in thermal vacuum as a function of the two-photon detuning Δ_T for $N=1$, $|M|=0$, $\delta=0$, $\Delta_0=\Delta=0$, $\xi_a=\xi_b=1$, $\gamma_1=\gamma_3=0.5$, and different γ_{13} : (—), $\gamma_{13}=0$; (---), $\gamma_{13}=0.5$.

that the coherence transfer rate γ_{13} tends to destroy the CPT effect when $\gamma_{13}=(\gamma_1\gamma_3)^{1/2}$ and $\gamma_1=\gamma_3$. In this case $\dot{\rho}_{AA}=0$, indicating that the population in the state $|A\rangle$ does not change in time and retains its initial value. The population oscillates between the states $|2\rangle$ and $|S\rangle$, which indicates that the three-level system effectively has been reduced to a two-level system, with the upper state $|2\rangle$ and lower state $|S\rangle$. This effect results in the Lorentzian seen in figure 2.

4.1.2. Reservoir at a finite temperature (broad-band thermal vacuum)

Now we consider the case of a thermal reservoir (broad-band thermal vacuum) interacting with the atomic system. In this case $N\neq 0$ and $|M|=0$. Figure 3 presents the stationary population of the state $|2\rangle$, when the atom is in the thermal reservoir with $N=1.0$. It is seen that for $\gamma_{13}=0$ the CPT effect is reduced compared with the previous case when $N=0$. This effect arises from the increased fluctuations presented in the thermal vacuum and may be explained by examining populations of the state $|A\rangle$ given by equation (16). For $N\neq 0$ the left-hand side of equation (16) can be equal to zero ($\dot{\rho}_{AA}=0$) only when $\bar{\rho}_{22}\neq 0$. Equation (16) also shows that for $\gamma_{13}=\gamma_1=\gamma_3$, $\xi_a=\xi_b$ and $\Delta_T=0$ the right-hand side of this equation is equal to zero, indicating that the population ρ_{AA} does not evolve in time ($\dot{\rho}_{AA}=0$). In this limit the population is trapped in $|2\rangle$ and $|S\rangle$ states independent of the temperature of the reservoir.

4.1.3. Squeezed reservoir (broad-band squeezed vacuum)

A squeezed reservoir or squeezed vacuum is characterized by strong correlations between two modes symmetrically located around the carrier frequency ω_s . When the squeezed vacuum is equally detuned from the atomic transition frequencies, then the squeezed correlations can lead to correlations between the atomic transitions. Let us first discuss the effect of the squeezed vacuum on the coherent population trapping. Figure 4 shows the dependence of the upper-state population on the two-photon detuning Δ_T in the case when the system is damped by a broad-band squeezed vacuum symmetrically coupled to the atomic transition

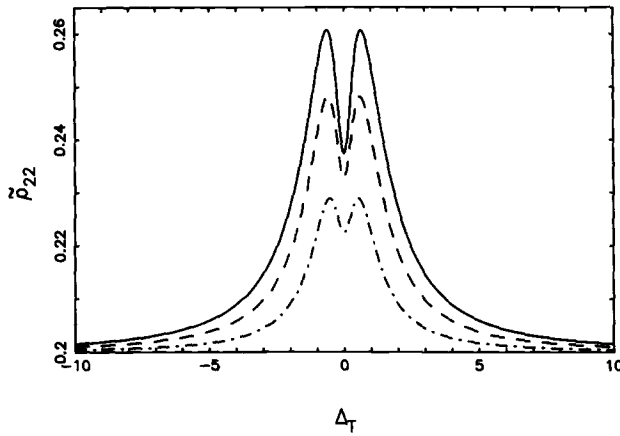


Figure 4. Stationary population of the upper state $|2\rangle$ in a squeezed vacuum as a function of the two-photon detuning Δ_T for $N=1$, $|M|^2=N(N+1)$, $\delta=0$, $\Delta_0=\Delta=0$, $\xi_a=\xi_b=1$, $\gamma_1=\gamma_3=0.5$, $\gamma_{13}=0$ and different phases φ_s : (—), $\varphi_s=0$; (---), $\varphi_s=\pi/2$; (-·-·-), $\varphi_s=\pi$.

frequencies and $\gamma_{13}=0$. The CPT effect is not further destroyed or improved compared with that in the thermal vacuum, but the coherence hole shows a strong dependence on the phase φ_s and is significantly more pronounced when $\varphi_s=0$. Figure 5 shows the upper-state population for the case when $\gamma_{13}\neq 0$. Here, as before for the ordinary and thermal vacua, there is no trapping effect. Depending on the phase φ_s the population in the state $|2\rangle$ can be significantly enhanced. A similar effect has been found in a two-level atom [5, 12]. There are, however, significant differences between the lambda three-level and two-level systems. It is well known that a two-level atom cannot be driven in a state of inversion under stationary conditions, regardless of the intensity of the driving field. The lambda three-level system is different as it can be driven into a state of inversion. Because $\rho_{AA}\approx 0$ and $\rho_{22}>0$ there is an inversion between the states $|2\rangle$ and $|A\rangle$. Moreover, for $\gamma_1=\gamma_3$ and $\varphi_s\neq 0$ or π there is an inversion between the states $|2\rangle$ and $|1\rangle$ or $|2\rangle$

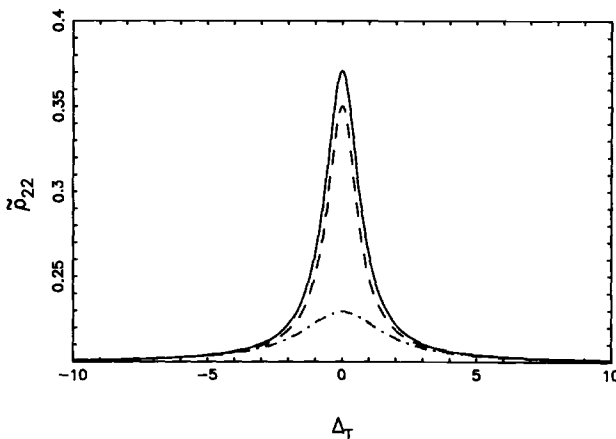


Figure 5. Same as in figure 4, but for $\gamma_{13}=0.5$.

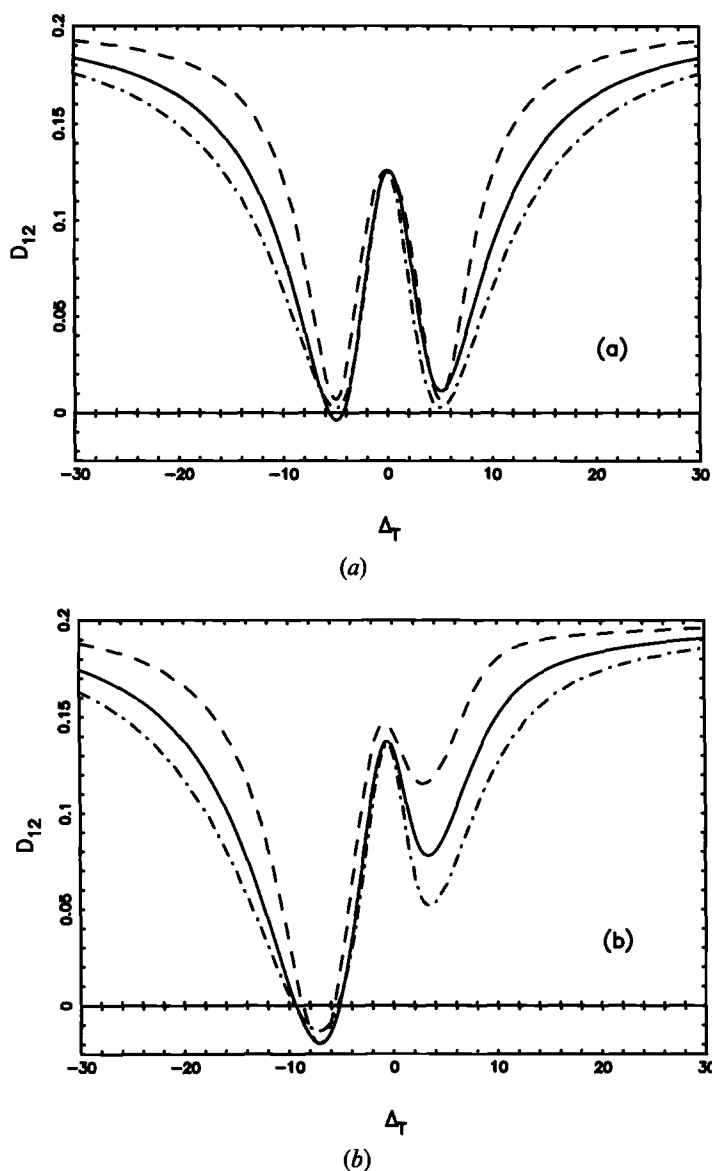


Figure 6. Population difference $D_{12} = \rho_{11} - \rho_{22}$ as a function of the two-photon detuning Δ_T for (a) $\delta = 0$, (b) $\delta = 5$, with $N = 1$, $|M|^2 = N(N + 1)$, $\Delta_0 = \Delta = 0$, $\xi_a = \xi_b = 10$, $\gamma_1 = \gamma_3 = 0.5$, $\gamma_{13} = 0$ and different phases φ_s : (---), $\varphi_s = 0$; (—), $\varphi_s = \pi/2$; (-·-·-), $\varphi_s = \pi$.

and $|3\rangle$. This is shown in figure 6(a), where we plot $D_{12} = \rho_{11} - \rho_{22}$ for $N = 1$, $\xi_a = \xi_b = 10$, $\gamma_1 = \gamma_3$, $\gamma_{13} = 0$, $\delta = 0$ and different phases φ_s . These graphs show that depending on the phase φ_s the population difference D_{12} can be negative for some values of Δ_T , indicating that there is an inversion between the allowed transitions of the lambda system. It is seen that the inversion appears only for $\varphi_s = \pi/2$. By changing the phase φ_s we can even switch the transition from non-inverted to inverted. The inversion can be enhanced when $\delta \neq 0$. This is shown in figure 6(b), where we plot D_{12} for the same parameters as in figure 6(a) but $\delta = 5$. This effect

is due to unequal population of the dressed states when $\delta \neq 0$ and/or $\varphi_s = \pi/2$ [12, 19].

For $\gamma_1 \neq \gamma_3$ there is an inversion even for $\delta = 0$ and $\varphi_s = 0$ or π . This is shown in figure 7, where we plot D_{12} for $N=1$, $\xi_a = \xi_b = 10$, $\gamma_{13} = 0$, $\gamma_3 = 9\gamma_1 = 0.9$, and different phases φ_s . It is evident that there is inversion between the states $|2\rangle - |1\rangle$, whereas the transition $|2\rangle - |3\rangle$ is not inverted. This effect has a simple physical interpretation; because the spontaneous emission in the $|2\rangle - |3\rangle$ transition is much faster than in the $|2\rangle - |1\rangle$ transition, the population oscillates between the states $|2\rangle - |3\rangle$ rather than $|2\rangle - |1\rangle$, leading to the inversion between $|2\rangle$ and $|1\rangle$.

4.2. Case when $\omega_a \neq \omega_b$ ($\Delta_0 \gg 1$) and $\omega_s = \frac{1}{2}(\omega_a + \omega_b)$ ($\Delta = 0$): steady-state solutions

Until now we have restricted our discussion on the steady-state solutions of the equations (13) to the case when both driving lasers have the same frequencies equal to the carrier frequency of the squeezed vacuum. In the case when $\Delta_0 \neq 0$ the coefficients of the equations of motion (13) are time dependent. However, when Δ_0 is significantly different from zero, the coefficients multiplied by $\exp(\pm i\Delta_0 t)$ are very small as they rapidly oscillate in time, and using the secular approximation we can ignore these terms in equation (13). It is interesting to note that, depending on ω_s , different terms will contribute to equations (13) after the secular approximation. When $\omega_s = \frac{1}{2}(\omega_a + \omega_b)$, then $\Delta = 0$ and, after dropping the rapidly oscillating terms, equations (13) reduce to

$$\begin{aligned}\dot{\rho}_{11} &= -N\gamma_1\rho_{11} + (N+1)\gamma_1\rho_{22} + \frac{1}{2}\xi_a(\rho_{12} + \rho_{21}), \\ \dot{\rho}_{22} &= N\gamma_3 + N(\gamma_1 - \gamma_3)\rho_{11} - [(N+1) + N\gamma_3]\rho_{22} - \frac{1}{2}\xi_a(\rho_{12} + \rho_{21}) - \frac{1}{2}\xi_b(\rho_{32} + \rho_{23}), \\ \dot{\rho}_{12} = \dot{\rho}_{21}^* &= -\{i(\Delta_T + \delta) + \frac{1}{2}[N\gamma_1 + (N+1)]\}\rho_{12} - \frac{1}{2}\xi_b\rho_{13} - \frac{1}{2}\xi_a(\rho_{11} - \rho_{22}) - M^*\gamma_{13}\rho_{23}, \\ \dot{\rho}_{32} = \dot{\rho}_{23}^* &= -\frac{1}{2}\xi_b + \{i(\Delta_T - \delta) - \frac{1}{2}[(N+1) + N\gamma_3]\}\rho_{32} - \frac{1}{2}\xi_a\rho_{31} + \frac{1}{2}\xi_b(2\rho_{22} + \rho_{11}) \\ &\quad - M^*\gamma_{13}\rho_{21}, \\ \dot{\rho}_{13} = \dot{\rho}_{31}^* &= -(2i\Delta_T + \frac{1}{2}N)\rho_{13} + \frac{1}{2}\xi_b\rho_{12} + \frac{1}{2}\xi_a\rho_{23}.\end{aligned}\quad (18)$$

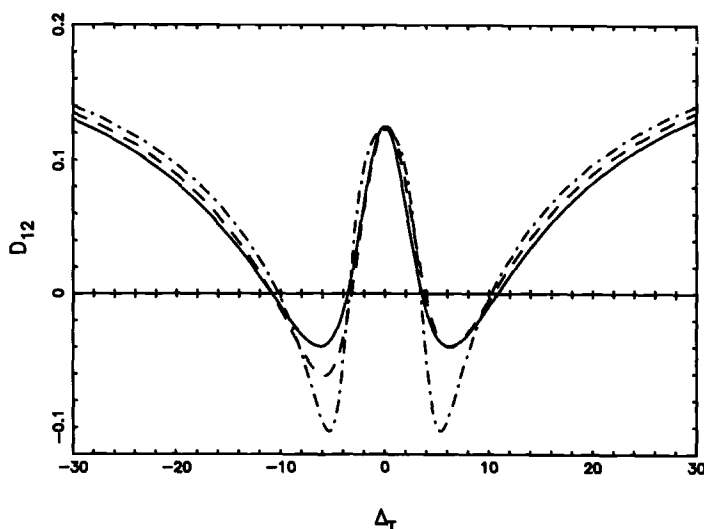


Figure 7. Same as in figure 6 (a), but $\gamma_3 = 9\gamma_1 = 0.9$.

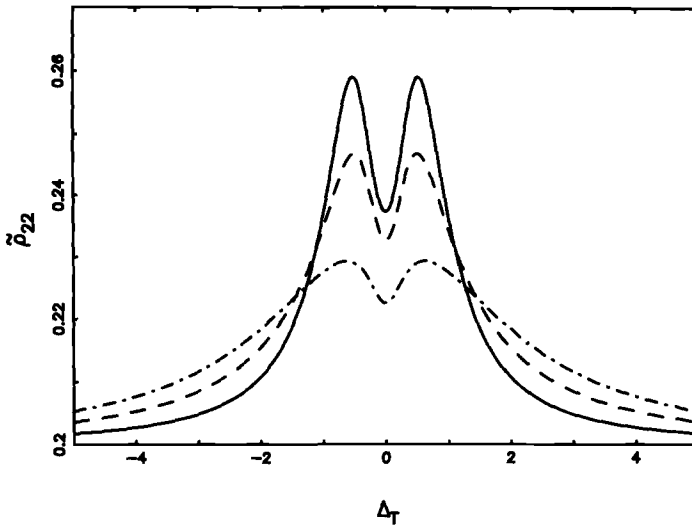


Figure 8. Stationary population of the upper state $|2\rangle$ as a function of Δ_T for $N=1$, $|M|^2 = N(N+1)$, $\xi_a = \xi_b = 1$, $\gamma_1 = \gamma_3 = \gamma_{13} = 0.5$, $\delta = 0$, $\Delta = 0$, $\Delta_0 \gg 1$ and different φ_s : (—), $\varphi_s = 0$; (---), $\varphi_s = \pi/2$; (-·-·-), $\varphi_s = \pi$.

It is seen that in this case the equations of motion for the density matrix elements depend on the degree of squeezing $|M|$ and the phase φ_s only when $\gamma_{13} \neq 0$; otherwise the equations (18) reduce to those of a thermal reservoir. Figure 8 shows the population of the upper state $|2\rangle$ as a function of Δ_T for $N=1$, $|M|^2 = N(N+1)$, $\xi_a = \xi_b = 1$, $\gamma_{13} = \gamma_1 = \gamma_3 = 0.5$, $\delta = 0$ and different phases φ_s . Here, in contrast with the case when both laser fields had the same frequency, the CPT effect is not destroyed when $\gamma_{13} \neq 0$. The coherence hole shows a strong dependence on the phase φ_s and is more pronounced when $\varphi_s = 0$.

4.3. Case where $\omega_s = \omega_a \neq \omega_b$ ($\Delta_0 \gg 1$): steady-state solutions

When the carrier frequency ω_s of the squeezed vacuum equals the frequency of one of the two driving laser fields, for example $\omega_s = \omega_a$, then $\Delta = \Delta_0$ and, after the secular approximation is made, equation (13) reduces to

$$\begin{aligned} \dot{\tilde{\rho}}_{11} &= -N\gamma_1\tilde{\rho}_{11} + (N+1)\gamma_1\tilde{\rho}_{22} + \frac{1}{2}\xi_a(\tilde{\rho}_{12} + \tilde{\rho}_{21}), \\ \dot{\tilde{\rho}}_{22} &= N\gamma_3 + N(\gamma_1 - \gamma_3)\tilde{\rho}_{11} - [(N+1) + N\gamma_3]\tilde{\rho}_{22} - \frac{1}{2}\xi_a(\tilde{\rho}_{12} + \tilde{\rho}_{21}) - \frac{1}{2}\xi_b(\tilde{\rho}_{32} + \tilde{\rho}_{23}), \\ \dot{\tilde{\rho}}_{12} = \dot{\tilde{\rho}}_{21}^* &= -\{i(\Delta_T + \delta) + \frac{1}{2}[N\gamma_1 + (N+1)]\}\tilde{\rho}_{12} - \frac{1}{2}\xi_b\tilde{\rho}_{13} - \frac{1}{2}\xi_a(\tilde{\rho}_{11} - \tilde{\rho}_{22}) - M^*\gamma_1\tilde{\rho}_{21}, \\ \dot{\tilde{\rho}}_{32} = \dot{\tilde{\rho}}_{23}^* &= -\frac{1}{2}\xi_b + \{i(\Delta_T - \delta) - \frac{1}{2}[(N+1) + N\gamma_3]\}\tilde{\rho}_{32} - \frac{1}{2}\xi_a\tilde{\rho}_{31} + \frac{1}{2}\xi_b(2\tilde{\rho}_{22} + \tilde{\rho}_{11}), \\ \dot{\tilde{\rho}}_{13} = \dot{\tilde{\rho}}_{31}^* &= -(2i\Delta_T + \frac{1}{2}N)\tilde{\rho}_{13} + \frac{1}{2}\xi_b\tilde{\rho}_{12} + \frac{1}{2}\xi_a\tilde{\rho}_{23}. \end{aligned} \quad (19)$$

In this case the degree of squeezing $|M|$ and the phase φ_s only occur in the equations for $\dot{\tilde{\rho}}_{12}$ and $\dot{\tilde{\rho}}_{21}$. Despite this the one-photon coherences $\tilde{\rho}_{32}$ and $\tilde{\rho}_{23}$ can be sensitive to the squeezed correlations M . This is shown in figure 9, where we plot the steady-state values of $|\tilde{\rho}_{32}|$ as a function of the two-photon detuning Δ_T .

for $N=1$, $|M|^2 = N(N+1)$, $\xi_a = \xi_b = 10$ and different values of the phase φ_s . This graph shows that the coherence $|\rho_{32}|$ strongly depends on the phase φ_s , despite the fact that the squeezing parameter M does not appear in the equation for ρ_{32} . This effect arises because through the driving field $|\Omega_b|$ the coherence $|\rho_{32}|$ is coupled to the population of the upper state $|2\rangle$, which on the other hand is coupled to the ρ_{12} coherence.

4.4. Case when $\omega_a \neq \omega_b$ ($\Delta_0 \approx 1$) and $\omega_s = \frac{1}{2}(\omega_a + \omega_b)$ ($\Delta = 0$) and $\gamma_{13} = 0$: oscillatory long-time solutions

In a general case when $\omega_a \neq \omega_b$ but Δ_0 is not too large, we cannot apply the secular approximation, the coefficients of the equation (13) are time dependent and the equations do not have simple analytical solutions. At long times the density matrix elements will have a constant term together with oscillatory terms at the various frequencies ($n\Delta_0 + m\Delta$) (n, m integers). However, we still can solve the system of equations (13) using, for example, continued-fraction techniques [28]. To illustrate this we restrict our calculations to the case of $\gamma_{13} = 0$ and $\Delta = 0$. In this limit the spontaneous emission transitions $|2\rangle \rightarrow |1\rangle$ and $|2\rangle \rightarrow |3\rangle$ are not correlated and the frequencies of the driving fields are symmetrically located around the carrier frequency of the squeezed vacuum. Performing the Laplace transform of equation (13), with $\gamma_{13} = 0$ and $\Delta = 0$ the equations can be written in a matrix form as

$$\mathbf{P}(s)\mathbf{X}(s) = \mathbf{X}_0(s), \quad (20)$$

where

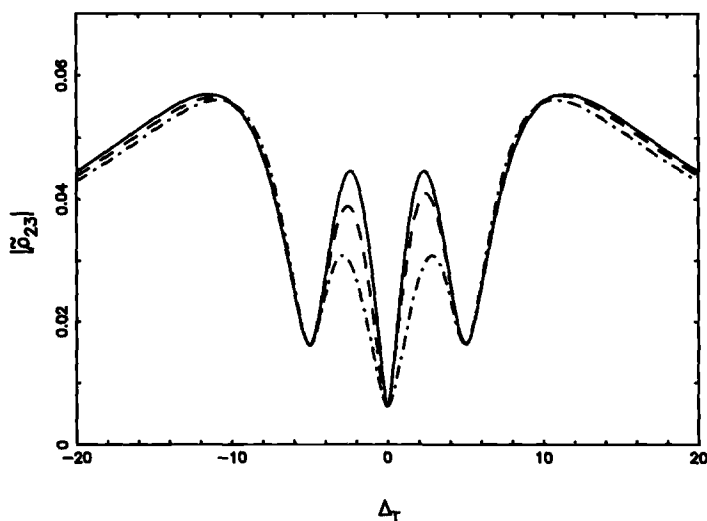


Figure 9. Stationary coherence $|\rho_{32}|$ as a function of Δ_T for $N=1$, $|M|^2 = N(N+1)$, $\delta=0$, $\gamma_1 = \gamma_3 = 0.5$, $\gamma_{13} = 0$, $\Delta_0 = \Delta \gg 1$, $\xi_a = \xi_b = 10$ and different phases φ_s : (—), $\varphi_s = 0$; (---), $\varphi_s = \pi/2$; (-·-·-), $\varphi_s = \pi$.

$$\mathbf{X}(s) = \begin{bmatrix} \vdots \\ \mathbf{X}^{(1)}(s) \\ \mathbf{X}^{(0)}(s) \\ \mathbf{X}^{(-1)}(s) \\ \vdots \end{bmatrix} \quad (21)$$

is an infinite-dimensional column vector composed of the subvectors

$$\mathbf{X}^{(n)}(s) = \begin{bmatrix} \sigma_{11}(s_n) \\ \sigma_{22}(s_n) \\ \sigma_{12}(s_n) \\ \sigma_{21}(s_n) \\ \sigma_{32}(s_n) \\ \sigma_{23}(s_n) \\ \sigma_{13}(s_n) \\ \sigma_{31}(s_n) \end{bmatrix} \quad (22)$$

containing Laplace transforms of the density matrix elements

$$\sigma_{ij}(s_n) = \int_0^\infty dt \exp(-s_n t) \rho_{ij}(t), \quad (23)$$

with $s_n = s + 2in\Delta_0$.

$\mathbf{P}(s)$ is an infinite-dimensional matrix composed of the 9×9 submatrices

$$\mathbf{P}(s) = \begin{bmatrix} \ddots & & & & & & & & \\ \mathbf{C} & \mathbf{A}(s_1) & \mathbf{B} & & & & & & \\ & \mathbf{C} & \mathbf{A}(s_0) & \mathbf{B} & & & & & \\ & & \mathbf{C} & \mathbf{A}(s_{-1}) & \mathbf{B} & & & & \\ & & & \ddots & \ddots & \ddots & \ddots & \ddots & \end{bmatrix}, \quad (24)$$

where

$$\mathbf{A}(s_n) = \begin{bmatrix} Z_1 & -(N+1)\gamma_1 & -\frac{1}{2}\xi_a & -\frac{1}{2}\xi_a & 0 & 0 & 0 & 0 \\ N(\gamma_3 - \gamma_1) & Z_2 & \frac{1}{2}\xi_a & \frac{1}{2}\xi_a & \frac{1}{2}\xi_b & \frac{1}{2}\xi_b & 0 & 0 \\ \frac{1}{2}\xi_a & -\frac{1}{2}\xi_a & Z_3 & 0 & 0 & 0 & \frac{1}{2}\xi_b & 0 \\ \frac{1}{2}\xi_a & -\frac{1}{2}\xi_a & 0 & Z_4 & 0 & 0 & 0 & \frac{1}{2}\xi_b \\ -\frac{1}{2}\xi_b & -\xi_b & 0 & 0 & Z_5 & 0 & 0 & \frac{1}{2}\xi_a \\ -\frac{1}{2}\xi_b & -\xi_b & 0 & 0 & 0 & Z_6 & \frac{1}{2}\xi_a & 0 \\ 0 & 0 & -\frac{1}{2}\xi_b & 0 & 0 & -\frac{1}{2}\xi_a & Z_7 & 0 \\ 0 & 0 & 0 & -\frac{1}{2}\xi_b & -\frac{1}{2}\xi_a & 0 & 0 & Z_8 \end{bmatrix} \quad (25)$$

with

$$\begin{aligned}
Z_1 &= s_n + N\gamma_1, & Z_2 &= s_n + N + 1 + N\gamma_3, \\
Z_3 &= s_n + i(\Delta_T + \delta) + \frac{1}{2}(N+1) + \frac{1}{2}N\gamma_1, \\
Z_4 &= s_n - i(\Delta_T + \delta) + \frac{1}{2}(N+1) + \frac{1}{2}N\gamma_1, \\
Z_5 &= s_n - i(\Delta_T - \delta) + \frac{1}{2}(N+1) + \frac{1}{2}N\gamma_3, \\
Z_6 &= s_n + i(\Delta_T - \delta) + \frac{1}{2}(N+1) + \frac{1}{2}N\gamma_3, \\
Z_7 &= s_n + 2i\Delta_T + \frac{1}{2}N, & Z_8 &= s_n - 2i\Delta_T + \frac{1}{2}N,
\end{aligned} \tag{26}$$

and the 9×9 matrices **C** and **B** have non-zero elements:

$$\begin{aligned}
C_{34} &= B_{43}^* = \gamma_1 M, \\
C_{56} &= B_{65}^* = \gamma_3 M.
\end{aligned} \tag{27}$$

In equation (20) $\mathbf{X}_0(s)$ is an infinite-dimensional vector composed of the sub-vectors containing initial values of the density matrix elements:

$$\mathbf{X}_0(s) = \begin{bmatrix} \vdots \\ \mathbf{X}_0^{(1)}(s) \\ \mathbf{X}_0^{(0)}(s) \\ \mathbf{X}_0^{(-1)}(s) \\ \vdots \end{bmatrix}, \tag{28}$$

where

$$\mathbf{X}_0^{(n)}(s) = \begin{bmatrix} \rho_{11}(0) \\ \rho_{22}(0) + N\gamma_3/s_n \\ \rho_{12}(0) \\ \rho_{21}(0) \\ \rho_{32}(0) - \frac{1}{2}\xi_b/s_n \\ \rho_{23}(0) - \frac{1}{2}\xi_b/s_n \\ \rho_{13}(0) \\ \rho_{31}(0) \end{bmatrix}. \tag{29}$$

It is seen from equation (24) that the presence of the squeezed vacuum results in coupling between $\mathbf{X}^{(n)}(s)$ and $\mathbf{X}^{(n \pm 1)}(s)$. This coupling is absent in a thermal vacuum and the matrix (24) has a simple diagonal form. In the squeezed vacuum the matrix (24) has a tridiagonal form.

The component of the vector $\mathbf{X}(s)$ can be easily found from equations (20)–(29) simply by matrix inversion. To invert the matrix **P**(*s*) we have to truncate the dimension of the vector $\mathbf{X}(s)$ at large numbers of terms. The validity of the truncation is ensured by requiring that $\mathbf{X}(s)$ does not change as the number of elements of the truncated vector $\mathbf{X}(s)$ was increased. The steady-state population of the state $|2\rangle$ is then found from the relation

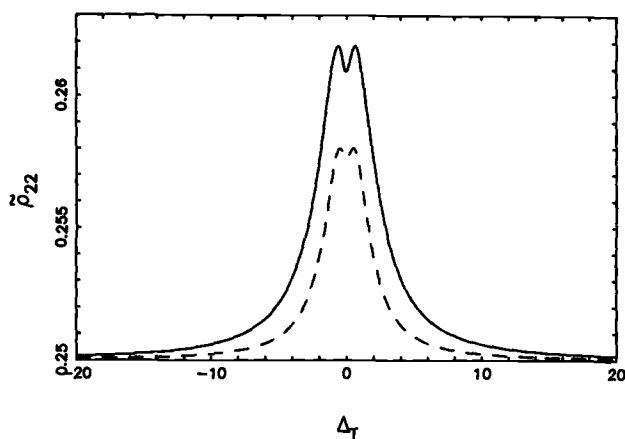


Figure 10. Stationary population ρ_{22} as a function of Δ_T for $N=2$, $\delta=0$, $\Delta=0$, $\Delta_0=0.5$, $\xi_a=\xi_b=0.5$, $\gamma_1=\gamma_3=0.5$, $\gamma_{13}=0$ and different degrees $|M|$ of squeezing: (—), $|M|=0$; (---), $|M|=[N(N+1)]^{1/2}$.

$$\rho_{22}(\infty) = \lim_{s \rightarrow \infty} [s\sigma_{22}(s)]. \quad (30)$$

Because the matrices **B** and **C** are complex conjugate, the determinant of the matrix **P**(*s*) is independent of the phase φ_s but depends on the degree of squeezing $|M|$. This is shown in figure 10, where we plot the stationary population of the state $|2\rangle$ as a function of the two-photon detuning Δ_T for $N=2$, $\Delta=\delta=0$, $\xi_a=\xi_b=0.5$, $\gamma_1=\gamma_3=0.5$, $\gamma_{13}=0$ and different values of the degree $|M|$ of squeezing. The population, in contrast with the case of the squeezed vacuum centred around one of the frequencies ω_a and ω_b of the driving fields, is insensitive to the phase φ_s but shows a strong dependence on the degree $|M|$ of squeezing. This rather surprising result arises because the population is calculated for the steady state ($t \rightarrow \infty$) so that only the stationary part of the time-dependent terms $|M \exp(\pm i n \Delta_0 t)|^2$ which are independent of the phase φ_s , contributes to the steady-state solution. Other non-stationary terms, which depend on the phase φ_s , oscillate with the frequency Δ_0 and average out over a long time.

5. Conclusions

In this paper we have investigated the effects of a broad-band squeezed vacuum on a three-level atom of the lambda configuration, which has also been coupled to two external coherent laser fields. We have derived the master equation for the system using the Born-Markov method adapted to the situation of a non-stationary reservoir. It is well known that multilevel atoms can display a much broader range of effects than their two-level counterparts as a result of the coherences induced between the states by the radiation, and the interference effects that can produce unexpected and sometimes counter-intuitive behaviours. In this paper we have focused mainly on the effect of a broad-band squeezed vacuum on the coherent population trapping. We have examined here the cases when the carrier frequency ω_s of the squeezed vacuum is

- (a) equal to both frequencies ω_a and ω_b of the driving fields,

- (b) equal to the average of the driving laser frequencies $\omega_s = \frac{1}{2}(\omega_a + \omega_b)$, which are themselves very different,
- (c) equal to the frequency of one of the two driving fields ($\omega_s = \omega_a$), and the other frequency ω_b is significantly different from ω_a and ω_s and
- (d) equal to the average of the driving field frequencies $\omega_s = \frac{1}{2}(\omega_a + \omega_b)$, which are themselves not very different.

We have shown that in case (a) the coefficients of the Bloch equations are time independent and stationary solutions for the populations and coherences are obtained by standard matrix methods. For the ordinary vacuum the usual coherent population trapping effect at two-photon resonance is obtained, with the upper-state population being zero. An unsqueezed thermal field partially destroys the trapping effect as the upper-state population is no longer zero at two-photon resonance. The squeezed vacuum has the effect of improving the trapping in that the coherence hole becomes more pronounced for some values of the relative phase between the coherent driving fields and the squeezed vacuum. The additional effects of a coherence transfer rate between the two optical coherences, which occurs for special choices of angular momentum quantum numbers have also been studied. The analysis have showed that the inclusion of this coherence transfer process destroys the coherent population trapping effect and reduces the three-level system to a two-level system. Moreover, we have shown that another feature that does not occur for two-level atoms, such as stationary population inversion between pairs of the atomic levels, depends on the squeezing parameters and can be enhanced for some values of the phase. In case (b) the CPT effect is not destroyed when the coherence transfer rate is included and the coherence hole shows a strong dependence on the phase owing to the coupling between the one-photon coherences. In case (c) the population-trapping effect shows similar behaviours as in case (a), but another unexpected effect appears. The optical coherence of the transition which is significantly detuned from the carrier frequency ω_s shows a strong dependence on the phase, despite the fact that the coherence is not directly affected by the squeezed vacuum. This effect is due to the coherence transfer between the atomic transitions through the common upper state $|2\rangle$. In case (d) the coefficients in the Bloch equations are dependent on time, thereby necessitating the use of continued-fraction methods. We have shown that in this case the coherent population-trapping effect is insensitive to the phase φ_s and only for not too large detunings depends on the degree $|M|$ of squeezing. When the detunings are large, the coherent population trapping reduces to that in the thermal vacuum field.

Acknowledgments

This work was supported in part by the Australian Research Council via a QEII Fellowship (Z.F.) and the Science and Engineering Research Council via a visiting Fellowship (B.J.D.). Helpful discussions with Dr S. Swain, Dr S. Barnett and Mr G. Yeoman are acknowledged. Thanks are due to Professor P. L. Knight for his hospitality at Imperial College, London, and to Ms S. Saunders for typing the manuscript.

Appendix A. Derivation of the master equation for a non-stationary reservoir

The master equation for the reduced density operator ρ of a small system S interacting with a non-stationary reservoir R can be derived using a generalization

of any of a number of traditional techniques, based on the Born-Markov approximation [26]. The time evolution of the density operator $W(t)$ of the system plus reservoir obeys the equation

$$i\hbar \frac{\partial}{\partial t} W^I(t) = [H_{\text{RS}}^I(t), W^I(t)], \quad (\text{A } 1)$$

where H_{RS} is the system-reservoir interaction, and the superscript I stands for operators in the interaction picture.

Formally integrating equation (A 1) gives

$$W^I(t) = W^I(0) + \frac{1}{i\hbar} \int_0^t dt' [H_{\text{RS}}^I(t'), W^I(t')]. \quad (\text{A } 2)$$

Substituting this solution into the right-hand side of equation (A 1), and taking the trace over the reservoir states of each side of equation (A 1), we get

$$i\hbar \frac{\partial}{\partial t} \rho^I(t) = \text{Tr}_{\text{R}} \left\{ [H_{\text{RS}}^I(t), W^I(0)] \right\} + \frac{1}{i\hbar} \int_0^t dt' \text{Tr}_{\text{R}} \{ [H_{\text{RS}}^I(t), [H_{\text{RS}}^I(t'), W^I(t')]] \}, \quad (\text{A } 3)$$

where $\rho(t) = \text{Tr}_{\text{R}} [W(t)]$ is the reduced density operator for the small system S.

In most situations of interest the system and reservoir are initially uncorrelated, that is

$$W^I(0) = \rho_{\text{R}}(0)\rho(0), \quad (\text{A } 4)$$

where $\rho_{\text{R}}(0)$ is the density operator for the reservoir at $t=0$.

We now employ the Born approximation, in which the atom-field interaction is supposed to be weak, and there is no effect of the system on the reservoir. In this approximation the reservoir does not change in time, and we substitute in the right-hand side of equation (A 3)

$$W^I(t) = \rho_{\text{R}}(0)\rho^I(t). \quad (\text{A } 5)$$

This amounts to treating the reservoir-system coupling as correct to the second order.

Under this approximation, and after changing the time variable to $t' = t - \tau$, equation (A 3) simplifies to

$$\begin{aligned} i\hbar \frac{\partial}{\partial t} \rho^I(t) = & \text{Tr}_{\text{R}} \{ [H_{\text{RS}}^I(t), \rho_{\text{R}}(0)\rho^I(0)] \} + \frac{1}{i\hbar} \int_0^t d\tau \text{Tr}_{\text{R}} \\ & \times \{ [H_{\text{RS}}^I(t), [H_{\text{RS}}^I(t-\tau), \rho_{\text{R}}(0)\rho^I(t-\tau)]] \}. \end{aligned} \quad (\text{A } 6)$$

It is possible to write the coupling Hamiltonian $H_{\text{RS}}(t)$ as a linear combination of products of the system and reservoir operators S_a and R_a respectively [26] so that, in the interaction picture,

$$H_{\text{RS}}^I(t) = \sum_a \tilde{S}_a(t) \tilde{R}_a(t), \quad (\text{A } 7)$$

where \tilde{S}_a and \tilde{R}_a indicate system and reservoir operators in the interaction picture for separated system and reservoir evolution.

Substituting equation (A 7) into equation (A 6), we obtain

$$\begin{aligned} i\hbar \frac{\partial}{\partial t} \rho^l(t) = & \sum_a \langle \tilde{R}_a(t) \rangle [\tilde{S}_a(t), \rho^l(0)] + \frac{1}{i\hbar} \sum_{ab} \int_0^t d\tau \langle \tilde{R}_a(t) \tilde{R}_b(t-\tau) \rangle [\tilde{S}_a(t), \tilde{S}_b(t-\tau) \rho^l(t-\tau)] \\ & + \frac{1}{i\hbar} \sum_{ab} \int_0^t d\tau \langle \tilde{R}_b(t-\tau) \tilde{R}_a(t) \rangle [\tilde{S}_b(t-\tau) \rho^l(t-\tau), \tilde{S}_a(t)], \end{aligned} \quad (\text{A } 8)$$

where

$$\begin{aligned} \langle \tilde{R}_a(t) \rangle &= \text{Tr}_{\mathbf{R}}[\rho_{\mathbf{R}}(0) \tilde{R}_a(t)], \\ \langle \tilde{R}_a(t_1) \tilde{R}_b(t_2) \rangle &= \text{Tr}_{\mathbf{R}}[\rho_{\mathbf{R}}(0) \tilde{R}_a(t_1) \tilde{R}_b(t_2)], \end{aligned} \quad (\text{A } 9)$$

are the first- and second-order reservoir correlation functions. Here we do not assume the reservoir is in a stationary state, where $\rho_{\mathbf{R}}(0)$ commutes with the reservoir Hamiltonian. In this general case the first-order correlation function depends on time and the second-order correlation function does not depend only on the time difference.

It is the properties of the correlation functions (A 9) and in particular that they decay to zero over a short correlation time τ_c , that is

$$\begin{aligned} \langle \tilde{R}_a(t) \rangle &\rightarrow 0, & t \gg \tau_c, \\ \langle \tilde{R}_a(t_1) \tilde{R}_b(t_2) \rangle &\rightarrow 0, & |t_1 - t_2| \gg \tau_c, \end{aligned} \quad (\text{A } 10)$$

which enables us to make the Markoff approximation. Let Γ^{-1} be the typical decay time over which matrix elements of $\rho^l(t)$ vary. Then, provided that

$$\Gamma \tau_c \ll 1, \quad (\text{A } 11)$$

we can make the Markoff approximation, namely we replace $\rho^l(t-\tau)$ by $\rho^l(t)$ in equation (A 8), since over the time scale in which $\langle \tilde{R}_a(t) \tilde{R}_b(t-\tau) \rangle$ and $\langle \tilde{R}_b(t-\tau) \tilde{R}_a(t) \rangle$ are non-zero, $\rho^l(t-\tau)$ would hardly have changed from $\rho^l(t)$. On the assumption that the time $t \gg \tau_c$, the first term in equation (A 8) can be ignored. In the usual treatment the term $\langle \tilde{R}_a(t) \rangle$ is put equal to zero via the device of subtracting $\text{Tr}_{\mathbf{R}}[H_{\text{RS}} \rho_{\mathbf{R}}(0)]$ from the coupling term H_{RS} and adding it to the system Hamiltonian, but this is not necessary.

Thus for $t \gg \tau_c$ the Markovian master equation in the interaction picture is

$$\frac{\partial}{\partial t} \rho^l(t) = - \sum_{ab} \omega_{ab}^+ [\tilde{S}_a(t), \tilde{S}_b(t) \rho^l(t)] + \sum_{ab} \omega_{ab}^- [\tilde{S}_a(t), \rho^l(t) \tilde{S}_b(t)], \quad (\text{A } 12)$$

where the reservoir spectral densities are given by

$$\omega_{ab}^+ = \frac{1}{\hbar^2} \int_0^t d\tau \exp[-i(\omega_b - i\varepsilon)\tau] \langle \tilde{R}_a(t) \tilde{R}_b(t-\tau) \rangle, \quad (\text{A } 13)$$

$$\omega_{ab}^- = \frac{1}{\hbar^2} \int_0^t d\tau \exp[-i(\omega_b - i\varepsilon)\tau] \langle \tilde{R}_b(t-\tau) \tilde{R}_a(t) \rangle, \quad (\text{A } 14)$$

and we have chosen the system operators S_b to have a simple time dependence:

$$\tilde{S}_b(t-\tau) = \tilde{S}_b(t) \exp(-i\omega_b\tau), \quad (\text{A } 15)$$

where ω_b are the transition frequencies of the system S. In the stationary-reservoir case, the two time correlation functions only depend on τ ; the integrals can be extended to $+\infty$, giving the time-independent reservoir spectral densities. In the general case the mathematically convenient decay factor $\exp(-\varepsilon\tau)$ can be added.

On transforming equation (A 12) to the Schrödinger picture, the master equation takes the following form:

$$\frac{\partial \rho}{\partial t} = \frac{1}{i\hbar} [H_s, \rho] - i \sum_{ab} \Delta_{ab} [S_a S_b, \rho] + \sum_{ab} \Gamma_{ab} \{ [S_b, \rho S_a] + [S_b \rho, S_a] \}, \quad t \gg \tau_c, \quad (\text{A } 16)$$

where

$$\Delta_{ab} = \frac{1}{2i} (\omega_{ab}^+ - \omega_{ba}^-) \quad (\text{A } 17)$$

is an extra contribution to the system Hamiltonian which leads to frequency shifts of the atomic levels, and

$$\Gamma_{ab} = \frac{1}{2} (\omega_{ab}^+ + \omega_{ba}^-) \quad (\text{A } 18)$$

are the relaxation (damping) coefficients. Note that, in general, Δ_{ab} and Γ_{ab} depend on time as we shall see for the specific problem treated here. Also, the master equation (A 16) is only valid for times long compared with the correlation time τ_c .

The system and reservoir operators can often be grouped in pairs S_a, S_a^+ and R_a, R_a^+ such that

$$\begin{aligned} S_a^+ &= (S_a)^\dagger, \\ R_a^+ &= (R_a)^\dagger, \\ \omega_a^+ &= -\omega_a. \end{aligned} \quad (\text{A } 19)$$

In this case, symmetry relations between the reservoir spectral densities can be found:

$$\begin{aligned} \omega_{a^+b^+}^+ &= (\omega_{ab}^-)^*, \\ \omega_{a^+b^+}^- &= (\omega_{ab}^+)^*. \end{aligned} \quad (\text{A } 20)$$

These relationships simplify the calculations of the Γ_{ab} and Δ_{ab} .

Appendix B. Derivation of master equation (9)

For the specific case of interest, the system is the three-level atom and the modes of the quantized reservoir are the electromagnetic field. Our master equation is the general form (A 16).

In order to calculate the reservoir spectral densities (A 13) and (A 14) we start with the explicit form of the reservoir operators obtained from equation (6):

$$\begin{aligned}\tilde{R}_1(t) &= \tilde{R}_2(t) = -\frac{1}{2}i\hbar \sum_{\lambda} [\Omega_{\lambda}^{(1)} a_{\lambda} \exp(-i\omega_{\lambda}t) - (\Omega_{\lambda}^{(1)})^* a_{\lambda}^{\dagger} \exp(i\omega_{\lambda}t)], \\ \tilde{R}_3(t) &= \tilde{R}_4(t) = -\frac{1}{2}i\hbar \sum_{\lambda} [\Omega_{\lambda}^{(3)} a_{\lambda} \exp(-i\omega_{\lambda}t) - (\Omega_{\lambda}^{(3)})^* a_{\lambda}^{\dagger} \exp(i\omega_{\lambda}t)],\end{aligned}\quad (\text{B } 1)$$

and obtain

$$\begin{aligned}\langle \tilde{R}_a(t) \tilde{R}_b(t-\tau) \rangle &= -\frac{1}{4}\hbar^2 \sum_{\lambda\mu} \Omega_{\lambda}^{(a)} \Omega_{\mu}^{(b)} \langle a_{\lambda} a_{\mu} \rangle \exp(i\omega_{\mu}\tau) \exp[-i(\omega_{\lambda} + \omega_{\mu})t] + \frac{1}{4}\hbar^2 \sum_{\lambda\mu} \Omega_{\lambda}^{(a)} \\ &\times \Omega_{\mu}^{(b)*} \langle a_{\lambda} a_{\mu}^{\dagger} \rangle \exp(-i\omega_{\mu}\tau) \exp[-i(\omega_{\lambda} - \omega_{\mu})t] + \frac{1}{4}\hbar^2 \sum_{\lambda\mu} (\Omega_{\lambda}^{(a)})^* \Omega_{\mu}^{(b)} \\ &\times \langle a_{\lambda}^{\dagger} a_{\mu} \rangle \exp(i\omega_{\mu}\tau) \exp[-i(\omega_{\lambda} - \omega_{\mu})t] - \frac{1}{4}\hbar^2 \sum_{\lambda\mu} (\Omega_{\lambda}^{(a)})^* (\Omega_{\mu}^{(b)})^* \\ &\times \langle a_{\lambda}^{\dagger} a_{\mu}^{\dagger} \rangle \exp(-i\omega_{\mu}\tau) \exp[i(\omega_{\lambda} + \omega_{\mu})t], \quad (a, b = 1, 3).\end{aligned}\quad (\text{B } 2)$$

It is seen from equation (B 2) that the reservoir spectral densities are dependent on the correlation functions of the reservoir mode operators. We assume that the reservoir is in a broad-band squeezed vacuum state. In this state it is characterized by the following expressions for the non-zero expectation values of the reservoir mode operators [4]:

$$\begin{aligned}\langle a_{\lambda} a_{\mu}^{\dagger} \rangle &= [N(\omega_{\lambda}) + 1] \text{ for } \omega_{\lambda} = \omega_{\mu}, \\ \langle a_{\lambda}^{\dagger} a_{\mu} \rangle &= N(\omega_{\lambda}) \text{ for } \omega_{\lambda} = \omega_{\mu}, \\ \langle a_{\lambda} a_{\mu} \rangle &= M(\omega_{\lambda}) \text{ for } \omega_{\lambda} + \omega_{\mu} = 2\omega_s, \\ \langle a_{\lambda}^{\dagger} a_{\mu}^{\dagger} \rangle &= M^*(\omega_{\lambda}) \text{ for } \omega_{\lambda} + \omega_{\mu} = 2\omega_s,\end{aligned}\quad (\text{B } 3)$$

where the parameter $M(\omega_{\lambda})$ characterizes squeezing such that $|M(\omega_{\lambda})|^2 \leq N(\omega_{\lambda})[N(2\omega_s - \omega_{\lambda}) + 1]$, and ω_s is the carrier frequency of the squeezed vacuum field. The parameter $N(\omega_{\lambda})$ is proportional to the number of photons in the field modes, which is governed by the Planck thermal distribution

$$N(\omega_{\lambda}) = \left[\exp\left(\frac{\hbar\omega_{\lambda}}{k_B T}\right) - 1 \right]^{-1}, \quad (\text{B } 4)$$

where k_B is the Boltzmann constant and T is the temperature of the squeezed 'vacuum' field.

The complex parameter $M(\omega_{\lambda}) = M(2\omega_s - \omega_{\lambda}) = |M(\omega_{\lambda})| \exp i\varphi_{\lambda}$, where $|M(\omega_{\lambda})|$ is the degree of squeezing and φ_s is the phase of the squeezed vacuum, characterizes the squeezing, that is the correlations between the field mode at frequency ω_{λ} and the mode at frequency $2\omega_s - \omega_{\lambda}$. We note that, to have a squeezed 'vacuum' ($|M| \neq 0$), we require $N > 0$ so that some photons are present in the squeezed vacuum field. Also, non-zero M implies that the reservoir density operator $\rho_R(0)$ cannot be a function of the reservoir Hamiltonian as it is for a stationary reservoir. Thus the squeezed vacuum is not a reservoir stationary state. The Markoff approximation applies since for a broad-band squeezed vacuum the band width Γ_s of $M(\omega_{\lambda})$ is large compared to Rabi frequencies and atomic decay rates.

With equations (B 2) and (B 3) the reservoir spectral densities (A 13) take the form

$$\begin{aligned} \omega_{ab}^+ = & \frac{1}{4} \sum_{\lambda} \Omega_{\lambda}^{(a)} (\Omega_{\lambda}^{(b)})^* [N(\omega_{\lambda}) + 1] \int_0^t d\tau \exp[-i(\omega_b + \omega_{\lambda} - i\varepsilon)\tau] + \frac{1}{4} \sum_{\lambda} (\Omega_{\lambda}^{(a)})^* \Omega_{\lambda}^{(b)} N(\omega_{\lambda}) \\ & \times \int_0^t d\tau \exp[-i(\omega_b - \omega_{\lambda} - i\varepsilon)\tau] - \frac{1}{4} \sum_{\lambda, \mu} {}^* \Omega_{\mu}^{(a)} \Omega_{\lambda}^{(b)} M(\omega_{\mu}) \exp(-2i\omega_s t) \int_0^t d\tau \\ & \times \exp[-i(-2\omega_s + \omega_{\mu} + \omega_b - i\varepsilon)\tau] - \frac{1}{4} \sum_{\lambda, \mu} {}^* \Omega_{\mu}^{(a)} {}^* \Omega_{\lambda}^{(b)} {}^* M^*(\omega_{\mu}) \exp(2i\omega_s t) \\ & \times \int_0^t d\tau \exp[-i(2\omega_s - \omega_{\mu} + \omega_b - i\varepsilon)\tau], \quad (a, b = 1, 3), \end{aligned} \quad (\text{B } 5)$$

and where the other cases can be obtained using equation (A 20). The sum over λ, μ with the * indicates that only terms such that $\omega_{\lambda} + \omega_{\mu} = 2\omega_s$ occur.

The master equation applies for $t \gg \tau_c$. Choosing ε sufficiently small that $\exp(-\varepsilon\tau_c) \ll 1$ the time integrals appearing in equation (B 5) are evaluated to give

$$\int_0^t d\tau \exp[-i(\Delta - i\varepsilon)\tau] = \frac{-i}{\Delta - i\varepsilon}, \quad (\text{B } 6)$$

which in the limit as $\varepsilon \rightarrow 0_+$ reduces to [26]

$$\lim_{\varepsilon \rightarrow 0_+} \left(\frac{-i}{\Delta - i\varepsilon} \right) \rightarrow \pi \delta(\Delta) - i \frac{P}{\Delta}, \quad (\text{B } 7)$$

where P is the principal Cauchy value.

With the above equations, we can express the spectral densities explicitly as

$$\begin{aligned} \omega_{ab}^+ = & \frac{1}{4} \pi \sum_{\lambda} \Omega_{\lambda}^{(a)} (\Omega_{\lambda}^{(b)})^* [N(\omega_{\lambda}) + 1] \delta(\omega_{\lambda} + \omega_b) + \frac{1}{4} \pi \sum_{\lambda} (\Omega_{\lambda}^{(a)})^* \Omega_{\lambda}^{(b)} N(\omega_{\lambda}) \delta(\omega_{\lambda} - \omega_b) \\ & - \frac{1}{4} \pi \sum_{\lambda} \Omega_{\lambda}^{(a)} \Omega_{\lambda}^{(b)} M(\omega_{\lambda}) \exp(-2i\omega_s t) \delta(2\omega_s - \omega_b - \omega_{\lambda}) - \frac{1}{4} \pi \sum_{\lambda} (\Omega_{\lambda}^{(a)})^* (\Omega_{\lambda}^{(b)})^* M^*(\omega_{\lambda}) \\ & \times \exp(2i\omega_s t) \delta(2\omega_s + \omega_b - \omega_{\lambda}) - \frac{1}{4} i P \sum_{\lambda} [N(\omega_{\lambda}) + 1] \frac{\Omega_{\lambda}^{(a)} (\Omega_{\lambda}^{(b)})^*}{\omega_{\lambda} + \omega_b} + \frac{1}{4} i P \sum_{\lambda} N(\omega_{\lambda}) \\ & \times \frac{(\Omega_{\lambda}^{(a)})^* \Omega_{\lambda}^{(b)}}{\omega_{\lambda} - \omega_b} - \frac{1}{4} i P \sum_{\lambda} M(\omega_{\lambda}) \exp(-2i\omega_s t) \frac{\Omega_{\lambda}^{(a)} \Omega_{\lambda}^{(b)}}{2\omega_s - \omega_b - \omega_{\lambda}} + \frac{1}{4} i P \sum_{\lambda} M^*(\omega_{\lambda}) \\ & \times \exp(2i\omega_s t) \frac{(\Omega_{\lambda}^{(a)})^* (\Omega_{\lambda}^{(b)})^*}{2\omega_s + \omega_b - \omega_{\lambda}}, \quad (a, b = 1, 3). \end{aligned} \quad (\text{B } 8)$$

Here the mode λ^* has frequency $2\omega_s - \omega_{\lambda}$. In a similar way we find that the spectral densities $\omega_{ab}^-(t)$ can be expressed explicitly as

$$\begin{aligned}
\omega_{ab}^-(t) = & \frac{1}{4}\pi \sum_{\mathbf{a}} (\Omega_{\mathbf{a}}^{(a)})^* \Omega_{\mathbf{a}}^{(b)} [N(\omega_{\mathbf{a}}) + 1] \delta(\omega_{\mathbf{a}} - \omega_b) + \frac{1}{4}\pi \sum_{\mathbf{a}} \Omega_{\mathbf{a}}^{(a)} (\Omega_{\mathbf{a}}^{(b)})^* N(\omega_{\mathbf{a}}) \delta(\omega_{\mathbf{a}} + \omega_b) \\
& - \frac{1}{4}\pi \sum_{\mathbf{a}} \Omega_{\mathbf{a}}^{(a)} \Omega_{\mathbf{a}}^{(b)*} M(\omega_{\mathbf{a}}) \exp(-2i\omega_s t) \delta(2\omega_s - \omega_b - \omega_{\mathbf{a}}) \\
& - \frac{1}{4}\pi \sum_{\mathbf{a}} (\Omega_{\mathbf{a}}^{(a)})^* (\Omega_{\mathbf{a}}^{(b)})^* M^*(\omega_{\mathbf{a}}) \exp(2i\omega_s t) \delta(2\omega_s + \omega_b - \omega_{\mathbf{a}}) + \frac{1}{4}iP \sum_{\mathbf{a}} [N(\omega_{\mathbf{a}}) + 1] \\
& \times \frac{(\Omega_{\mathbf{a}}^{(a)})^* \Omega_{\mathbf{a}}^{(b)}}{\omega_{\mathbf{a}} - \omega_b} - \frac{1}{4}iP \sum_{\mathbf{a}} N(\omega_{\mathbf{a}}) \frac{\Omega_{\mathbf{a}}^{(a)} (\Omega_{\mathbf{a}}^{(b)})^*}{\omega_{\mathbf{a}} + \omega_b} - \frac{1}{4}iP \sum_{\mathbf{a}} M(\omega_{\mathbf{a}}) \exp(-2i\omega_s t) \\
& \times \frac{\Omega_{\mathbf{a}}^{(a)} \Omega_{\mathbf{a}}^{(b)*}}{2\omega_s - \omega_b - \omega_{\mathbf{a}}} + \frac{1}{4}iP \sum_{\mathbf{a}} M^*(\omega_{\mathbf{a}}) \exp(2i\omega_s t) \frac{(\Omega_{\mathbf{a}}^{(a)})^* (\Omega_{\mathbf{a}}^{(b)})^*}{2\omega_s + \omega_b - \omega_{\mathbf{a}}}, \quad (a, b = 1, 3).
\end{aligned} \tag{B 9}$$

From equation (6) the system operators S_1, \dots, S_4 are given terms of the atomic operators for the $|1\rangle-|2\rangle$ and $|3\rangle-|2\rangle$ transitions, and in the interaction picture we have

$$\begin{aligned}
\tilde{S}_1(t) &= S_1^+ \exp(i\omega_1 t), \\
\tilde{S}_2(t) &= S_1^- \exp(-i\omega_1 t), \\
\tilde{S}_3(t) &= S_3^+ \exp(i\omega_3 t), \\
\tilde{S}_4(t) &= S_3^- \exp(-i\omega_3 t),
\end{aligned} \tag{B 10}$$

where $\omega_1 = -\omega_2 = \omega_{21}$ and $\omega_3 = \omega_{23} = -\omega_4$ are the transition frequencies between the states $|1\rangle-|2\rangle$ and $|3\rangle-|2\rangle$ respectively, whereas $S_1^+ = (S_1^-)^\dagger = |2\rangle\langle 1|$ and $S_3^+ = (S_3^-)^\dagger = |2\rangle\langle 3|$ are the atomic operators. Using equation (B 10), we can calculate the spectral densities ω_{ij}^+ and ω_{ij}^- . We find that

$$\begin{aligned}
\omega_{11}^-(t) &= \omega_{22}^+(t)^* = \omega_{12}^+(t)^* = \omega_{21}^-(t) \\
&= \frac{1}{4}\pi \sum_{\mathbf{a}} \{ (\Omega_{\mathbf{a}}^{(1)})^* \Omega_{\mathbf{a}}^{(1)} [N(\omega_{\mathbf{a}}) + 1] \delta(\omega_{\mathbf{a}} - \omega_1) - \Omega_{\mathbf{a}}^{(1)} \Omega_{\mathbf{a}}^{(1)*} M(\omega_{\mathbf{a}}) \\
&\quad \times \exp(-2i\omega_s t) \delta(2\omega_s - \omega_1 - \omega_{\mathbf{a}}) \} \\
&\quad + \frac{1}{4}iP \sum_{\mathbf{a}} \left([N(\omega_{\mathbf{a}}) + 1] \frac{(\Omega_{\mathbf{a}}^{(1)})^* \Omega_{\mathbf{a}}^{(1)}}{\omega_{\mathbf{a}} - \omega_1} - N(\omega_{\mathbf{a}}) \frac{\Omega_{\mathbf{a}}^{(1)} (\Omega_{\mathbf{a}}^{(1)})^*}{\omega_{\mathbf{a}} + \omega_1} + M^*(\omega_{\mathbf{a}}) \exp(2i\omega_s t) \right. \\
&\quad \times \left. \frac{(\Omega_{\mathbf{a}}^{(1)})^* (\Omega_{\mathbf{a}}^{(1)})^*}{2\omega_s + \omega_1 - \omega_{\mathbf{a}}} - M(\omega_{\mathbf{a}}) \exp(-2i\omega_s t) \frac{\Omega_{\mathbf{a}}^{(1)} \Omega_{\mathbf{a}}^{(1)*}}{2\omega_s - \omega_1 - \omega_{\mathbf{a}}} \right),
\end{aligned} \tag{B 11}$$

$$\begin{aligned}
\omega_{12}^-(t) &= \omega_{21}^+(t)^* = \omega_{11}^+(t)^* = \omega_{22}^-(t) \\
&= \frac{1}{4}\pi \sum_{\mathbf{a}} [\Omega_{\mathbf{a}}^{(1)} (\Omega_{\mathbf{a}}^{(2)})^* N(\omega_{\mathbf{a}}) \delta(\omega_{\mathbf{a}} - \omega_1) \\
&\quad - (\Omega_{\mathbf{a}}^{(1)})^* (\Omega_{\mathbf{a}}^{(2)})^* M^*(\omega_{\mathbf{a}}) \exp(2i\omega_s t) \delta(2\omega_s - \omega_1 - \omega_{\mathbf{a}})] \\
&\quad + \frac{1}{4}iP \sum_{\mathbf{a}} \left([N(\omega_{\mathbf{a}}) + 1] \frac{(\Omega_{\mathbf{a}}^{(1)})^* \Omega_{\mathbf{a}}^{(2)}}{\omega_{\mathbf{a}} + \omega_1} - N(\omega_{\mathbf{a}}) \frac{\Omega_{\mathbf{a}}^{(1)} (\Omega_{\mathbf{a}}^{(2)})^*}{\omega_{\mathbf{a}} - \omega_1} \right. \\
&\quad \times \left. + M^*(\omega_{\mathbf{a}}) \exp(2i\omega_s t) \frac{(\Omega_{\mathbf{a}}^{(1)})^* (\Omega_{\mathbf{a}}^{(2)})^*}{2\omega_s - \omega_1 - \omega_{\mathbf{a}}} - M(\omega_{\mathbf{a}}) \exp(-2i\omega_s t) \frac{\Omega_{\mathbf{a}}^{(1)} \Omega_{\mathbf{a}}^{(2)*}}{2\omega_s + \omega_1 - \omega_{\mathbf{a}}} \right),
\end{aligned} \tag{B 12}$$

$$\begin{aligned}
\omega_{13}^-(t) &= \omega_{23}^-(t) = \omega_{24}^+(t)^* = \omega_{14}^+(t)^* \\
&= \frac{1}{4}\pi \sum_{\mathbf{a}} \{ (\Omega_{\mathbf{a}}^{(1)})^* \Omega_{\mathbf{a}}^{(3)} [N(\omega_{\mathbf{a}}) + 1] \delta(\omega_{\mathbf{a}} - \omega_3) - \Omega_{\mathbf{a}}^{(1)} \Omega_{\mathbf{a}}^{(3)*} M(\omega_{\mathbf{a}}) \\
&\quad \times \exp(-2i\omega_s t) \delta(2\omega_s - \omega_3 - \omega_{\mathbf{a}}) \} + \frac{1}{4}iP \sum_{\mathbf{a}} \left([N(\omega_{\mathbf{a}}) + 1] \frac{(\Omega_{\mathbf{a}}^{(1)})^* \Omega_{\mathbf{a}}^{(3)}}{\omega_{\mathbf{a}} - \omega_3} - N(\omega_{\mathbf{a}}) \right. \\
&\quad \times \frac{\Omega_{\mathbf{a}}^{(1)} (\Omega_{\mathbf{a}}^{(3)})^*}{\omega_{\mathbf{a}} + \omega_3} + M^*(\omega_{\mathbf{a}}) \exp(2i\omega_s t) \frac{(\Omega_{\mathbf{a}}^{(1)})^* (\Omega_{\mathbf{a}}^{(3)})^*}{2\omega_s + \omega_3 - \omega_{\mathbf{a}}} - M(\omega_{\mathbf{a}}) \\
&\quad \left. \times \exp(-2i\omega_s t) \frac{\Omega_{\mathbf{a}}^{(1)} \Omega_{\mathbf{a}}^{(3)*}}{2\omega_s - \omega_3 - \omega_{\mathbf{a}}} \right), \tag{B 13}
\end{aligned}$$

$$\begin{aligned}
\omega_{14}^-(t) &= \omega_{24}^-(t) = \omega_{23}^+(t)^* = \omega_{13}^+(t)^* \\
&= \frac{1}{4}\pi \sum_{\mathbf{a}} [(\Omega_{\mathbf{a}}^{(1)}) (\Omega_{\mathbf{a}}^{(4)})^* N(\omega_{\mathbf{a}}) \delta(\omega_{\mathbf{a}} - \omega_3) - (\Omega_{\mathbf{a}}^{(1)})^* (\Omega_{\mathbf{a}}^{(4)})^* M^*(\omega_{\mathbf{a}}) \\
&\quad \times \exp(2i\omega_s t) \delta(2\omega_s - \omega_3 - \omega_{\mathbf{a}})] + \frac{1}{4}iP \sum_{\mathbf{a}} \left([N(\omega_{\mathbf{a}}) + 1] \frac{(\Omega_{\mathbf{a}}^{(1)})^* \Omega_{\mathbf{a}}^{(4)}}{\omega_{\mathbf{a}} + \omega_3} \right. \\
&\quad - N(\omega_{\mathbf{a}}) \frac{\Omega_{\mathbf{a}}^{(1)} (\Omega_{\mathbf{a}}^{(4)})^*}{\omega_{\mathbf{a}} - \omega_3} + M^*(\omega_{\mathbf{a}}) \exp(2i\omega_s t) \frac{(\Omega_{\mathbf{a}}^{(1)})^* (\Omega_{\mathbf{a}}^{(4)})^*}{2\omega_s - \omega_3 - \omega_{\mathbf{a}}} - M(\omega_{\mathbf{a}}) \\
&\quad \left. \times \exp(-2i\omega_s t) \frac{\Omega_{\mathbf{a}}^{(1)} \Omega_{\mathbf{a}}^{(4)*}}{2\omega_s + \omega_3 - \omega_{\mathbf{a}}} \right), \tag{B 14}
\end{aligned}$$

$$\begin{aligned}
\omega_{31}^-(t) &= \omega_{41}^-(t) = \omega_{42}^+(t)^* = \omega_{32}^+(t)^* \\
&= \frac{1}{4}\pi \sum_{\mathbf{a}} \{ (\Omega_{\mathbf{a}}^{(3)})^* \Omega_{\mathbf{a}}^{(1)} [N(\omega_{\mathbf{a}}) + 1] \delta(\omega_{\mathbf{a}} - \omega_1) - \Omega_{\mathbf{a}}^{(3)} \Omega_{\mathbf{a}}^{(1)*} M(\omega_{\mathbf{a}}) \\
&\quad \times \exp(-2i\omega_s t) \delta(2\omega_s - \omega_1 - \omega_{\mathbf{a}}) \} \\
&\quad + \frac{1}{4}iP \sum_{\mathbf{a}} \left([N(\omega_{\mathbf{a}}) + 1] \frac{(\Omega_{\mathbf{a}}^{(3)})^* \Omega_{\mathbf{a}}^{(1)}}{\omega_{\mathbf{a}} - \omega_1} \right. \\
&\quad - N(\omega_{\mathbf{a}}) \frac{\Omega_{\mathbf{a}}^{(3)} (\Omega_{\mathbf{a}}^{(1)})^*}{\omega_{\mathbf{a}} - \omega_1} + M^*(\omega_{\mathbf{a}}) \exp(2i\omega_s t) \frac{(\Omega_{\mathbf{a}}^{(3)})^* (\Omega_{\mathbf{a}}^{(1)})^*}{2\omega_s + \omega_1 - \omega_{\mathbf{a}}} - M(\omega_{\mathbf{a}}) \\
&\quad \left. \times \exp(-2i\omega_s t) \frac{\Omega_{\mathbf{a}}^{(3)} \Omega_{\mathbf{a}}^{(1)*}}{2\omega_s - \omega_1 - \omega_{\mathbf{a}}} \right), \tag{B 15}
\end{aligned}$$

$$\begin{aligned}
\omega_{32}^-(t) &= \omega_{42}^-(t) = \omega_{41}^+(t)^* = \omega_{31}^+(t)^* \\
&= \frac{1}{4}\pi \sum_{\mathbf{a}} [\Omega_{\mathbf{a}}^{(3)} (\Omega_{\mathbf{a}}^{(2)})^* N(\omega_{\mathbf{a}}) \delta(\omega_{\mathbf{a}} - \omega_1) - (\Omega_{\mathbf{a}}^{(3)})^* (\Omega_{\mathbf{a}}^{(2)})^* M^*(\omega_{\mathbf{a}}) \\
&\quad \times \exp(2i\omega_s t) \delta(2\omega_s - \omega_1 - \omega_{\mathbf{a}})] + \frac{1}{4}iP \sum_{\mathbf{a}} \left([N(\omega_{\mathbf{a}}) + 1] \frac{(\Omega_{\mathbf{a}}^{(3)})^* \Omega_{\mathbf{a}}^{(2)}}{\omega_{\mathbf{a}} + \omega_1} \right. \\
&\quad - N(\omega_{\mathbf{a}}) \frac{\Omega_{\mathbf{a}}^{(3)} (\Omega_{\mathbf{a}}^{(2)})^*}{\omega_{\mathbf{a}} - \omega_1} + M^*(\omega_{\mathbf{a}}) \exp(2i\omega_s t) \frac{(\Omega_{\mathbf{a}}^{(3)})^* (\Omega_{\mathbf{a}}^{(2)})^*}{2\omega_s - \omega_1 - \omega_{\mathbf{a}}} - M(\omega_{\mathbf{a}}) \\
&\quad \left. \times \exp(-2i\omega_s t) \frac{\Omega_{\mathbf{a}}^{(3)} \Omega_{\mathbf{a}}^{(2)*}}{2\omega_s + \omega_1 - \omega_{\mathbf{a}}} \right), \tag{B 16}
\end{aligned}$$

$$\begin{aligned}
\omega_{33}^-(t) &= \omega_{43}^-(t) = \omega_{44}^+(t)^* = \omega_{34}^+(t)^* \\
&= \frac{1}{4}\pi \sum_{\lambda} \{ (\Omega_{\lambda}^{(3)})^* (\Omega_{\lambda}^{(3)}) [N(\omega_{\lambda}) + 1] \delta(\omega_{\lambda} - \omega_3) - \Omega_{\lambda}^{(3)} \Omega_{\lambda}^{(3)*} M(\omega_{\lambda}) \\
&\quad \times \exp(-2i\omega_s t) \delta(2\omega_s - \omega_3 - \omega_{\lambda}) \} + \frac{1}{4}iP \sum_{\lambda} \left([N(\omega_{\lambda}) + 1] \frac{(\Omega_{\lambda}^{(3)})^* \Omega_{\lambda}^{(3)}}{\omega_{\lambda} - \omega_3} \right. \\
&\quad - N(\omega_{\lambda}) \frac{\Omega_{\lambda}^{(3)} (\Omega_{\lambda}^{(3)})^*}{\omega_{\lambda} + \omega_3} + M^*(\omega_{\lambda}) \exp(2i\omega_s t) \frac{(\Omega_{\lambda}^{(3)})^* (\Omega_{\lambda}^{(3)})^*}{2\omega_s + \omega_3 - \omega_{\lambda}} - M(\omega_{\lambda}) \\
&\quad \left. \times \exp(-2i\omega_s t) \frac{\Omega_{\lambda}^{(3)} \Omega_{\lambda}^{(3)*}}{2\omega_s - \omega_3 - \omega_{\lambda}} \right), \tag{B 17}
\end{aligned}$$

$$\begin{aligned}
\omega_{34}^-(t) &= \omega_{43}^+(t)^* = \omega_{33}^+(t)^* = \omega_{44}^-(t) \\
&= \frac{1}{4}\pi \sum_{\lambda} [\Omega_{\lambda}^{(3)} (\Omega_{\lambda}^{(4)})^* N(\omega_{\lambda}) \delta(\omega - \omega_3) - (\Omega_{\lambda}^{(3)})^* (\Omega_{\lambda}^{(4)})^* M^*(\omega_{\lambda}) \\
&\quad \times \exp(2i\omega_s t) \delta(2\omega_s - \omega_3 - \omega_{\lambda})] + \frac{1}{4}iP \sum_{\lambda} \left([N(\omega_{\lambda}) + 1] \frac{(\Omega_{\lambda}^{(3)})^* \Omega_{\lambda}^{(4)}}{\omega_{\lambda} + \omega_3} \right. \\
&\quad - N(\omega_{\lambda}) \frac{\Omega_{\lambda}^{(3)} (\Omega_{\lambda}^{(4)})^*}{\omega_{\lambda} - \omega_3} + M^*(\omega_{\lambda}) \exp(2i\omega_s t) \frac{(\Omega_{\lambda}^{(3)})^* (\Omega_{\lambda}^{(4)})^*}{2\omega_s - \omega_3 - \omega_{\lambda}} - M(\omega_{\lambda}) \\
&\quad \left. \times \exp(-2i\omega_s t) \frac{\Omega_{\lambda}^{(3)} \Omega_{\lambda}^{(4)*}}{2\omega_s + \omega_3 - \omega_{\lambda}} \right), \tag{B 18}
\end{aligned}$$

where $\Omega_{\lambda}^{(1)}$, $\Omega_{\lambda}^{(3)}$ are given in equations (7) and (8), and $\Omega_{\lambda}^{(2)} = \Omega_{\lambda}^{(1)}$, $\Omega_{\lambda}^{(4)} = \Omega_{\lambda}^{(3)}$. In obtaining (B 11) to (B 18) it is assumed that the bandwidth Γ_s for $M(\omega_{\lambda})$ is small compared to ω_1, ω_3 .

With the spectral densities (B 11)–(B 18) and making the rotating-wave approximation, in which we can ignore all terms oscillating with higher frequencies, $2\omega_i$, $\omega_i + \omega_j$, the general master equation (A 16) adopted to the case of the three-level lambda system takes the following form:

$$\begin{aligned}
\frac{\partial}{\partial t} \rho^l(t) &= - \sum_{i,j} [M_{ij} + i\Delta M_{ij}] \{ [S_i^+, \rho^l S_j^+] - [S_i^+, S_j^+ \rho^l] \} \exp[-i(2\omega_s - \omega_i - \omega_j)t] \\
&\quad - \sum_{i,j} [M_{ij}^* - i\Delta M_{ij}^*] \{ [S_i^-, \rho^l S_j^-] - [S_i^-, S_j^- \rho^l] \} \exp[i(2\omega_s - \omega_i - \omega_j)t] \\
&\quad + \sum_{i,j} \Gamma_{ij}^+ \{ [S_i^-, \rho^l S_j^+] - [S_j^+, S_i^- \rho^l] \} \exp[-i(\omega_i - \omega_j)t] \\
&\quad + \sum_{i,j} \Gamma_{ij}^- \{ [S_i^+, \rho^l S_j^-] - [S_j^-, S_i^+ \rho^l] \} \exp[i(\omega_i - \omega_j)t] \\
&\quad + i \sum_{i,j} \Delta_{ij}^- [S_i^- S_j^+, \rho^l] \exp[-i(\omega_i - \omega_j)t] \\
&\quad + i \sum_{i,j} \Delta_{ij}^+ [S_i^+ S_j^-, \rho^l] \exp[i(\omega_i - \omega_j)t], \tag{B 19}
\end{aligned}$$

where $i, j = 1, 3$ and

$$\begin{aligned}
M_{ij} &= \frac{\pi}{8} \sum_{\mathbf{A}} M(\omega_{\mathbf{A}}) \{ \Omega_{\mathbf{A}}^{(i)} \Omega_{\mathbf{A}}^{(j)} \delta(\omega_{\mathbf{A}} - 2\omega_s + \omega_i) + \Omega_{\mathbf{A}}^{(i)} \Omega_{\mathbf{A}}^{(j)*} \delta(\omega_{\mathbf{A}} - 2\omega_s + \omega_j) \}, \\
\Delta M_{ij} &= \frac{P}{8} \sum_{\mathbf{A}} M(\omega_{\mathbf{A}}) \left\{ \frac{\Omega_{\mathbf{A}}^{(i)} \Omega_{\mathbf{A}}^{(j)}}{(2\omega_s - \omega_{\mathbf{A}} - \omega_i)} + \frac{\Omega_{\mathbf{A}}^{(i)} \Omega_{\mathbf{A}}^{(j)*}}{(2\omega_s - \omega_{\mathbf{A}} - \omega_j)} \right\}, \\
\Gamma_{ij}^+ &= \frac{\pi}{4} \sum_{\mathbf{A}} (N(\omega_{\mathbf{A}}) + 1) (\Omega_{\mathbf{A}}^{(i)} \Omega_{\mathbf{A}}^{(j)} \frac{1}{2} \{ \delta(\omega_{\mathbf{A}} - \omega_i) + \delta(\omega_{\mathbf{A}} - \omega_j) \}), \\
\Gamma_{ij}^- &= \frac{\pi}{4} \sum_{\mathbf{A}} N(\omega_{\mathbf{A}}) \Omega_{\mathbf{A}}^{(i)} (\Omega_{\mathbf{A}}^{(j)})^* \frac{1}{2} \{ \delta(\omega_{\mathbf{A}} - \omega_i) + \delta(\omega_{\mathbf{A}} - \omega_j) \}, \\
\Delta_{ij} &= \frac{P}{4} \sum_{\mathbf{A}} \left\{ (N(\omega_{\mathbf{A}}) + 1) \Omega_{\mathbf{A}}^{(i)} (\Omega_{\mathbf{A}}^{(j)})^* \frac{1}{2} \left(\frac{1}{\omega_{\mathbf{A}} + \omega_i} + \frac{1}{\omega_{\mathbf{A}} + \omega_j} \right) \right. \\
&\quad \left. - N(\omega_{\mathbf{A}}) (\Omega_{\mathbf{A}}^{(i)})^* \Omega_{\mathbf{A}}^{(j)} \frac{1}{2} \left(\frac{1}{\omega_{\mathbf{A}} - \omega_i} + \frac{1}{\omega_{\mathbf{A}} - \omega_j} \right) \right\}, \\
\Delta_{ij}^+ &= \frac{P}{4} \sum_{\mathbf{A}} \left\{ (N(\omega_{\mathbf{A}}) + 1) \Omega_{\mathbf{A}}^{(i)} (\Omega_{\mathbf{A}}^{(j)})^* \frac{1}{2} \left(\frac{1}{\omega_{\mathbf{A}} - \omega_i} + \frac{1}{\omega_{\mathbf{A}} - \omega_j} \right) \right. \\
&\quad \left. - N(\omega_{\mathbf{A}}) (\Omega_{\mathbf{A}}^{(i)})^* \Omega_{\mathbf{A}}^{(j)} \frac{1}{2} \left(\frac{1}{\omega_{\mathbf{A}} + \omega_i} + \frac{1}{\omega_{\mathbf{A}} + \omega_j} \right) \right\} \quad (\text{B } 20)
\end{aligned}$$

The parameters Γ_{ii}^+ and Γ_{ii}^- ($i=1, 3$), which appear in the master equation (B 19), are the intensity-dependent decay rates for the atomic transitions, Γ_{ij}^+ and Γ_{ij}^- ($i \neq j$) are the intensity-dependent coherence transfer rates, whereas Δ_{ij}^N , and $\Delta_{ij}^{(N+1)}$ are the intensity-dependent Lamb shifts and M_{ij} and ΔM_{ij} are squeezing rate parameters.

Using the definitions (7) and (8) for the one-photon Rabi frequencies, we can evaluate the parameters Γ_{ij}^+ ($N=0$) $\equiv \Gamma_{ij}$, which are the spontaneous decay ($i=j$) and coherence transfer rates ($i \neq j$). This gives:

$$\Gamma_{11} = \frac{|\mu_{12}|^2 \omega_{21}^3}{6\pi\hbar\epsilon_0 c^3}, \quad (\text{B } 21)$$

$$\Gamma_{33} = \frac{|\mu_{32}|^2 \omega_{23}^3}{6\pi\hbar\epsilon_0 c^3}, \quad (\text{B } 22)$$

and

$$\Gamma_{13} = \Gamma_{31}^* = \frac{\mu_{12} \mu_{32}^*}{12\pi\hbar\epsilon_0 c^3} (\omega_{21}^3 + \omega_{23}^3). \quad (\text{B } 23)$$

References

- [1] LOUDON, R., and KNIGHT, P. L., (editors), 1987, *J. mod. Optics*, **34**(6/7), special issue; KIMBLE, H. J., and WALLS, D. F., (editors), 1987, *J. opt. Soc. Am. B*, **4**(10), special issue; TEICH, M. C., and SALEH, B. E. A., 1989, *Quant. Optics*, **1**, 153; ZAHEER, K., and ZUBAIRY, M. S., 1990, *Adv. at molec. opt. Phys.*, **28**, 143.
- [2] PARKINS, A. S., 1993, *Adv. chem. Phys.*, **85**, 607.

- [3] POLZIK, E. S., CARRI, J., and KIMBLE, H. J., 1992, *Phys. Rev. Lett.*, **68**, 3020; *Appl. Phys. B*, **55**, 279.
- [4] GARDINER, C. W., 1986, *Phys. Rev. Lett.*, **56**, 1917.
- [5] CARMICHAEL, H. J., LANE, A. S., and WALLS, D. F., 1987, *J. mod. Optics*, **34**, 821; 1987, *Phys. Rev. Lett.*, **58**, 2539.
- [6] RITSCH, H., and ZOLLER, P. 1987, *Optics Commun.*, **64**, 523; AN, S., and SARGENT, M., III, 1989, *Phys. Rev. A*, **39**, 3998; ZHANG, W., and TAN, W., 1988, *Optics Commun.*, **69**, 135.
- [7] FICEK, Z., and DALTON, B. J., 1993, *Optics Commun.*, **102**, 231.
- [8] MILBURN, G. J., 1986, *Phys. Rev. A*, **34**, 4882.
- [9] FORD, G. W., and O'CONNELL, R. F., 1987, *J. opt. Soc. Am. B*, **4**, 1710.
- [10] PALMA, G. M., and KNIGHT, P. L., 1989, *Optics Commun.*, **73**, 131.
- [11] FICEK, Z., 1993, *J. mod. Optics*, **40**, 2333.
- [12] SMART, S., and SWAIN, S., 1993, *Phys. Rev. A*, **48**, R50; SMYTH, W. S., and SWAIN, S., 1994, *Optics Commun.*, **112**, 91.
- [13] FICEK, Z., SMYTH, W. S., and SWAIN, S., 1994, *Optics Commun.*, **110**, 555.
- [14] FICEK, Z., and DRUMMOND, P. D., 1991, *Phys. Rev. A*, **43**, 6247, 6258.
- [15] BUZEK, V., KNIGHT, P. L., and KUDRYAVTSEV, I. K., 1991, *Phys. Rev. A*, **44**, 1931.
- [16] FICEK, Z., and DRUMMOND, P. D., 1993, *Europhys. Lett.*, **24**, 455.
- [17] JAGATAP, B. N., LAWANDE, Q. V., and LAWANDE, S. V., 1991, *Phys. Rev. A*, **43**, 535.
- [18] JOSHI, A., and PURI, R. R., 1992, *Phys. Rev. A*, **45**, 2025.
- [19] SMART, S., and SWAIN, S., 1992, *Quant. Optics*, **4**, 281; 1993, *J. mod. Optics*, **40**, 1939.
- [20] ORRIOLS, G., 1979, *Nuovo Cim.*, **53**, 5.
- [21] DALTON, B. J., and KNIGHT, P. L., 1982, *J. Phys. B*, **15**, 399.
- [22] MANKA, A. S., DOSS, H. M., NARDUCCI, L. M., RU, P., and OPPO, G. L., 1991, *Phys. Rev. A*, **43**, 3748.
- [23] PARKINS, A. S., and GARDINER, C. W., 1988, *Phys. Rev. A*, **37**, 3867.
- [24] RITSCH, H., and ZOLLER, P., 1988, *Phys. Rev. Lett.*, **61**, 1087; 1988, *Phys. Rev. A*, **38**, 4657.
- [25] PARKINS, A. S., 1990, *Phys. Rev. A*, **42**, 4352, 6873; G. YEOMAN, and BARNETT, S., 1994, (to be published).
- [26] COHEN-TANNOUDJI, C., 1977, *Frontiers in Laser Spectroscopy*, edited by R. Balian, S. Haroche and S. Liberman (Amsterdam: North-Holland), p. 33; AGARWAL, G. S., 1974, *Quantum Optics*, Springer Tracts in Modern Physics, Vol. 70, edited by G. Höhler (Berlin: Springer), p. 88; LOUISELL, W. H., 1973, *Quantum Statistical Properties of Radiation* (New York: Wiley), chapter 6.
- [27] HEGERFELDT, G. C., and PLENIO, M. B., 1993, *Phys. Rev. A*, **47**, 2186; LI, G.-X., and PENG, J. S., 1994, *Phys. Lett. A*, **189**, 449; CARDIMONA, D. A., 1990, *Phys. Rev. A*, **41**, 5016.; CARDIMONA, D. A., RAYMER, M. C., and STROUD, C. R., JR., 1982, *J. Phys. B*, **15**, 55.
- [28] RISKEN, H., 1984, *The Fokker-Planck Equation* (Berlin: Springer), chapter 9.